FUNDAMENTALS OF FLUID FILM THRUST BEARING OPERATION AND MODELING

Minhui He
Machinery Specialist
BRG Machinery Consulting, LLC
North Garden, Virginia, USA

James M. Byrne
Machinery Specialist
BRG Machinery Consulting, LLC
North Garden, Virginia, USA

Minhui He is a Machinery Specialist with BRG Machinery Consulting LLC, in North Garden, Virginia. His responsibilities include vibration troubleshooting, rotordynamic analysis, as well as bearing and seal analysis and design. He is also conducting research on rotordynamics and hydrodynamic bearings.
Dr. He received his B.S. degree (Chemical Machinery Engineering, 1994) from Sichuan University. From 1996 to 2003, he conducted research on fluid film journal bearings in the ROMAC Laboratories at the University of Virginia, receiving his Ph.D. (Mechanical and Aerospace Engineering, 2003). He is a member of ASME and the advisory committee for the Texas A&M Asia Turbomachinery and Pump Symposium.

James M. Byrne is a member of the BRG Machinery Consulting team in North Garden, Virginia. BRG provides a wide variety of machinery consulting services including design and analysis, selection, auditing, commissioning and troubleshooting. Mr. Byrne began his career designing internally geared centrifugal compressors for Carrier in Syracuse, New York. He continued his career at Pratt and Whitney aircraft engines and became a technical leader for rotordynamics. Later, Mr. Byrne became a program manager for Pratt and Whitney Power Systems managing the development of new gas turbine products. From 2001 to 2007, he was President of Rotating Machinery Technology, a manufacturer of tilting pad bearings.
Mr. Byrne holds a BSME degree from Syracuse University, an MSME degree from the University of Virginia, and an MBA from Carnegie Mellon University. He is a member of the API 613 special purpose gear and API 617 centrifugal compressor task forces.

ABSTRACT

Widely used in turbomachinery, the fluid film thrust bearing is critical to the overall reliability of a machine. Their design complexity and application severity continue to increase, making it challenging for the plant engineer to evaluate their reliability. This tutorial first provides practical knowledge on their basic physics, including hydrodynamic pressure generation, temperature rise due to internal viscous shearing and elastic deformation, as well as how those aspects interact with each other during operation. Examples are given to demonstrate how common design and operational parameters affect a bearing's key performance parameters, such as the minimum film thickness and pad temperature. Then, this tutorial reviews the analytical models used to simulate the various physical aspects. The state of the art techniques for modeling important aspects are presented, along with discussions on their capabilities and limitations. Also covered in this tutorial are subjects including flooded versus evacuated housing design and direct lubrication, as well as a brief discussion on dynamics.

INTRODUCTION

The objectives of this tutorial are to provide each student the following with respect to fluid film thrust bearings:

- A basic understanding of their physics and operational considerations

- A basic understanding of their modeling fundamentals

- The knowledge to better interpret more advanced papers and topics

- A good reference source for the future

This tutorial is not:

- A design guideline. We do not intend to teach you how to design a bearing for any particular application.

- A bearing primer. We expect the student to have a basic understanding of fluid film bearings, their use and basic operation. We do not describe all types of bearings, nor the evolution of their design.

- A journal bearing tutorial. We focus solely on thrust bearings, although many of the topics and much of the physics is also applicable to journal bearings. The authors presented a separate tutorial on the journal bearings in 2016 (He *at al.* (2016)).

The authors' primary audience is the plant machinery engineer evaluating new versus old designs to fix their problems, as well as central engineering machinery specialists in charge of selecting and auditing bearing designs for new machinery. The goal is to prepare these individuals to ask good questions of those performing a bearing design or analysis. Plant engineers must understand the limits of any analysis so that they can manage risk and assess alternatives. Bearing designers will also find the material useful in supplementing their expertise. These individuals must understand the underlying physics behind the computer program they are running. They, too, must understand the limitations and risks associated with their analysis. They must understand all of the options and inputs to their bearing code, plus understand what the output is telling them.

Why are the fundamentals of thrust bearing operation and modeling important?

- Designs are more and more aggressive with less margin for error.

- Loads and speeds continue to increase in new machinery.

- While the basic fluid dynamics of fluid film bearings are well understood, secondary effects such as elastic deformations, heat transfer to the solids and turbulence are less well established.

- Innovation breeds new designs and technologies that cause the old analysis methods to fall short.

- The desire for lower power loss and lower oil consumption.

- The desire for improved reliability forces better understanding.

- The cost of redesign (trial and error) is enormous.

- The cost of a plant outage is greater.

- You cannot test everything!

How does a poor bearing design manifest itself?

- Wear due to low film thickness, perhaps with low speed bearings or due to contaminants.

- High bearing metal temperatures, eventually leading to bearing failure

- High machinery axial displacement or axial vibrations.

- Excessive power loss

- Excessive oil consumption

What are some common operational limits?

- Surface speeds: up to 170 m/s (555 ft/s).

- Unit or specific load, W_U: up to 5 MPa (725 psi).

- Bearing metal temperature for Babbitt lined bearings:

    - A typical design limit is 100 °C (212 °F)
    - A typical mechanical run test or shop test limit is 100 °C (212 °F)
    - A typical field alarm limit is 110 °C (230 °F)
    - A typical field trip limit is 121 °C (250 °F)
    - Alternative materials and lubricants can run above 121 °C (250 °F).

- Minimum film thickness: A conservative value is 25 μm (0.001 in). The API standard for centrifugal pumps (API 610 (11th Edition)) establishes a minimum film thickness of 8 μm (0.0003 in). Discussions on minimum film thickness can be found in Martin & Garner (1973).

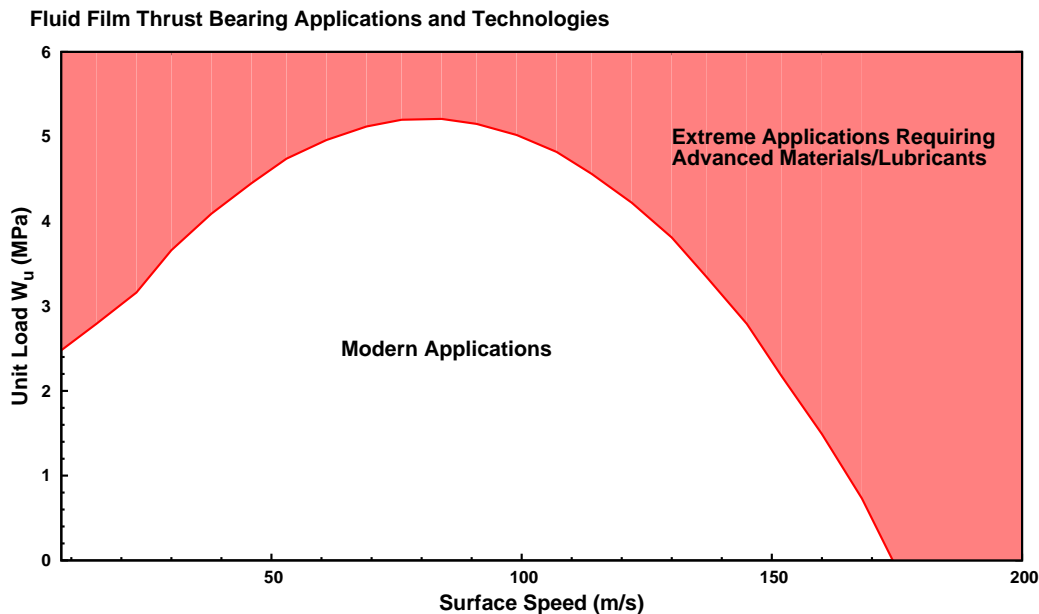**Fluid Film Thrust Bearing Applications and Technologies**

Figure 1: Thrust bearing operational limits

Figure 1 provides the operational limits of fluid film thrust bearings in terms of surface speed (at the outer diameter of the thrust bearing) and unit load (applied load divided by the total bearing pad area). This plot assumes Babbitted bearings using ISO VG 32 mineral oil, and should only be used as an initial point of reference. It should not replace a thorough analysis.

At low surface speeds, operation is limited by the minimum film thickness. The bearing's ability to generate hydrodynamic pressure is directly proportional to the relative motion provided by surface speed. Therefore, low speeds limit hydrodynamic pressure, resulting in thin films. As surface speed increases, unit load reaches a maximum. Beyond this maximum, unit load

is reduced due to the effects of viscous shearing. At high surface speeds, viscous shearing of the oil generates significant heat, pushing the bearing surface material (Babbitt) and the oil (ISO VG 32 mineral oil assumed here) to their operating temperature limits. Remember, however, that load capacity increases with speed. With sufficiently low applied loads and high speeds, the operating film thickness of a fluid film thrust bearing can become quite large. This differs from journal bearings where the operating film thickness can never surpass the bearing's radial clearance. As a result, the operating speed limit is somewhat higher for thrust bearings than for journal bearings.

Operation can be extended into the red region of extreme applications with alternate bearing materials and synthetic lube oil. Higher speeds can also be achieved with lower viscosity fluids, but the load capacity would simultaneously be reduced.

The first section of this tutorial begins with a discussion of the operational aspects of fluid film bearings. Bearing geometrical aspects are discussed and the basic physics of fluid film bearing operation are developed. The second section uses what was learned in the operational section and describes the means by which one can model or predict fluid film bearing behavior.

OPERATION

A commonly used tilting pad thrust bearing is schematically shown in Figure 2. In this example, the pads are assembled in the retainer and each pad can tilt circumferentially and radially about a spherical pivot on its back. The sector shaped pad has an arc length of θ in the circumferential direction. Its radial dimension (width) is $(D_O - D_I)/2$. The pivot location is defined by its circumferential and radial offsets as $\phi_c = \beta/\theta$ and $\phi_r = (D_P - D_I)/(D_O - D_I)$, respectively. A pad of 0.5 circumferential offset is said to have *central pivot*.

The size of a thrust bearing is represented by its outer diameter D_O. For example, a 267 mm (10.5 in) thrust bearing means its outer diameter is 267 mm. The loading magnitude is often expressed as the specific or unit load given by the following:

$$W_U = \frac{F_a}{N_P \times A_P} \tag{1}$$

where F_a is the axial load in N (lbf), N_P is the number of pads and A_P is the area of each pad in mm^2 (in^2). Therefore, W_U is the load relative to the bearing area that is available to carry it, and has the unit of MPa (psi).

To handle thrust load in both directions, there are usually two thrust bearings on both sides of the thrust collar. In this setup, only one of the two bearings are loaded at any given operating point. The loaded side is called the active bearing and the other side is called inactive or slack bearing.
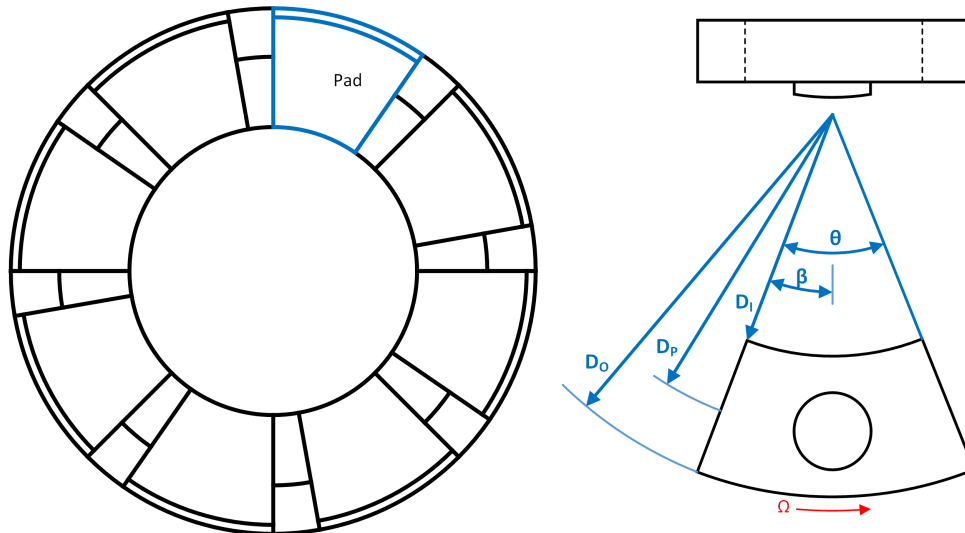

Figure 2: Schematics of tilting pad thrust bearing

Principle of Hydrodynamic Lubrication
The understanding of hydrodynamic lubrication was pioneered by Beauchamp Tower and Osborne Reynolds in late 1800s. While studying the friction losses in railroad bearings (Tower (1883), Tower (1885)), Tower encountered a persistent oil leak from the oiler hole supplying the single axial groove in his bearing, shown in Figure 3(a). He realized that the lubricating oil was becoming pressurized after the plug was blown out of the hole. Tower modified the design such that the oil was

supplied through two axial grooves, allowing him to install pressure gauges on the bearing surface. One example of his pressure measurements are shown in Figure 3(b). Integrating the pressure, Tower found that the fluid force equaled the load he applied on the bearing. In 1886, Osborne Reynolds theoretically confirmed Tower's observations that the pressure in the lubricant film carries the external load and separates the solid surfaces (Reynolds (1886)). Reynolds also identified the three ingredients necessary for hydrodynamic lubrication: *viscous fluid*, *a converging clearance* and *relative motion*.
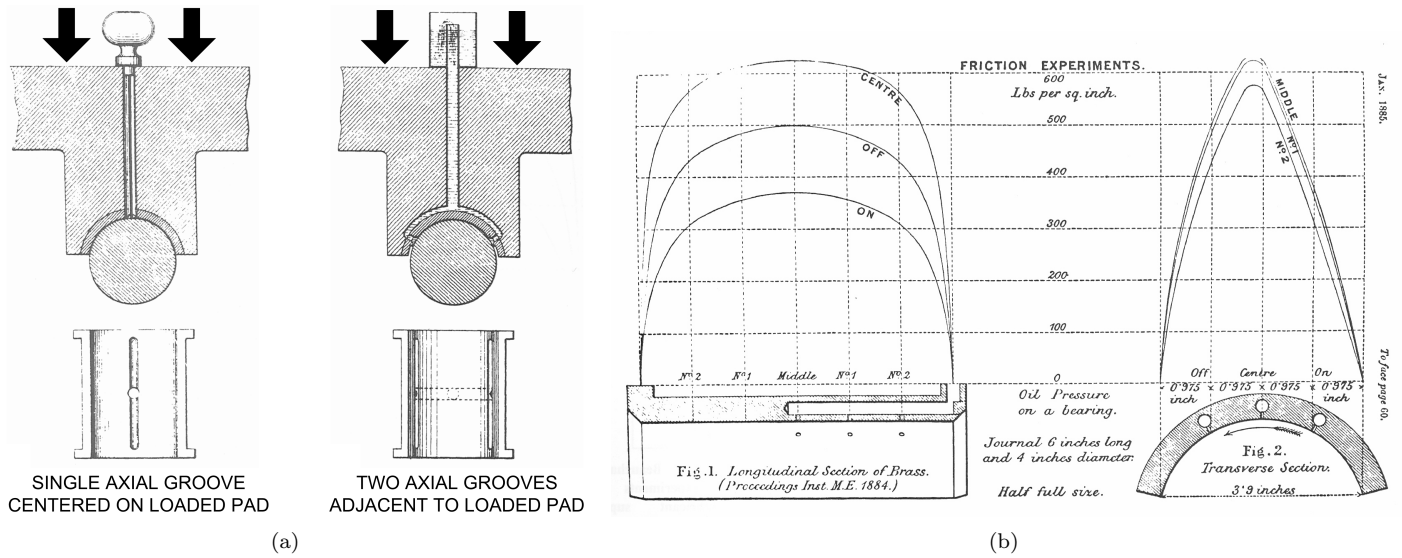

Figure 3: Tower's experiments on bearings, Tower (1883)

Physically, the viscous lubricant is dragged into the bearing clearance by the moving surface. If the clearance is converging, the fluid is squeezed by the two surfaces, generating hydrodynamic pressure. Figure 4 shows the velocity and pressure profiles in the lubricant film assuming laminar flow. The velocity profile is the combination of the linear shear (Couette) flow and parabolic pressure driven (Poiseuille) flow.

If there were no pressure, the velocity profile would be linear and its average across the thin film would be a constant of $U/2$, where U is the surface velocity. Since the film thickness h is decreasing along the flow path, the condition of flow continuity or mass conservation could not be satisfied ($\dot{m} = \rho (U/2) h$, where the varying h leads to varying $\dot{m}$). To maintain flow continuity, hydrodynamic pressure must be generated. As shown in the figure, before the peak pressure, the pressure gradient is adverse, and thus, the overall velocity profile is the linear profile *minus* the parabolic profile. In other words, the pressure tends to slow down the flow in this relatively large clearance region. Past the peak pressure in the smaller clearance region, the pressure driven flow is *added* to the shear flow, increasing the total velocity. Flow continuity is achieved by this varying velocity due to the hydrodynamic pressure ($\dot{m} = \rho u h$, where both u and h vary to keep $\dot{m}$ constant). In a real bearing, where the flow field is three dimensional, the hydrodynamic pressure also results in leakage across the inner and outer diameters of a thrust pad.
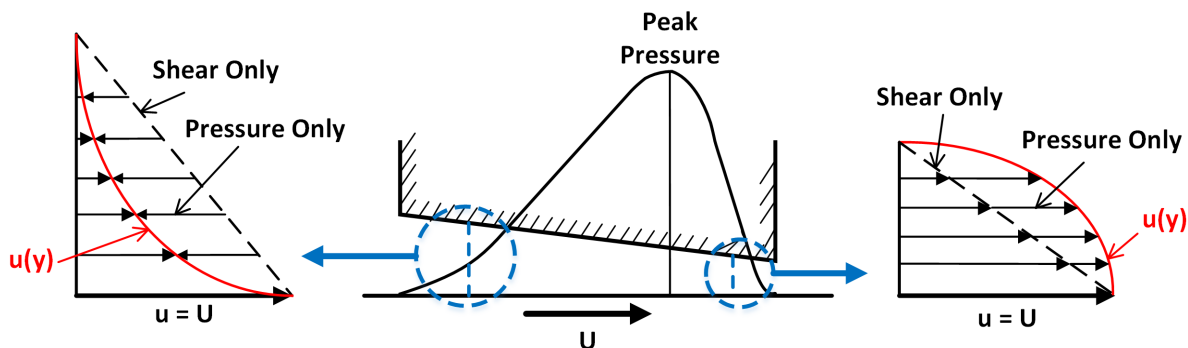

Figure 4: Pressure and velocity profiles in a converging clearance

What happens if the clearance is diverging? In a diverging clearance, the incompressible lubricant cannot expand to fill the increasing space along the flow path. In most applications where the bearing is exposed to the atmosphere, the lubricant film will rupture and the ambient air will enter the clearance, resulting in two-phase flow. This phenomenon is called cavitation. In the cavitation region, there is no hydrodynamic pressure and heat generation due to internal viscous shearing is substantially reduced. Cavitation is very common in journal bearings and can happen in heavily loaded thrust bearings. However, unlike pump cavitation, bearing cavitation does not cause damage and is usually not a concern.

The general trends of hydrodynamic lubrication can be summarized as the following:

- Higher viscosity leads to higher hydrodynamic pressure.

- Higher relative velocity leads to higher hydrodynamic pressure.

- For a single application, the slope of the converging wedge has an optimum value. A slope that is too shallow does not produce sufficient squeeze effect. However, an overly steep slope cannot effectively generate pressure either due to the exceedingly large clearance near the inlet.

Fixed Geometry Versus Tilting Pad

Thrust bearings are usually classified as fixed geometry or tilting pad. Figure 5 shows a simple flat land fixed geometry bearing. The surfaces of the pads and the thrust collar are in parallel by design. Due to the lack of obvious converging wedge, this bearing is only suitable to carry a light thrust load (< 0.5 MPa or 75 psi) (Wilcock & Booser (1957), Whalen (1996)). The source of its load carrying capacity was extensively debated in history because it cannot be explained by isothermal lubrication theory. Nowadays, it is generally agreed that it is the thermal distortion of the pads that produces small convergence in operation.
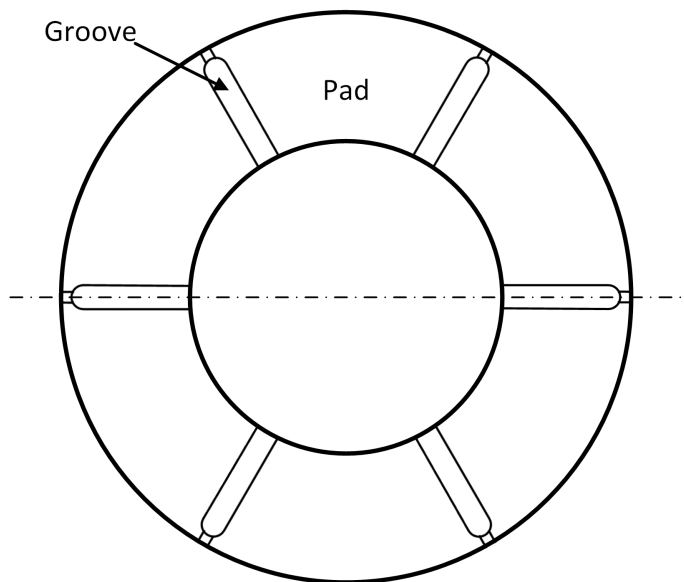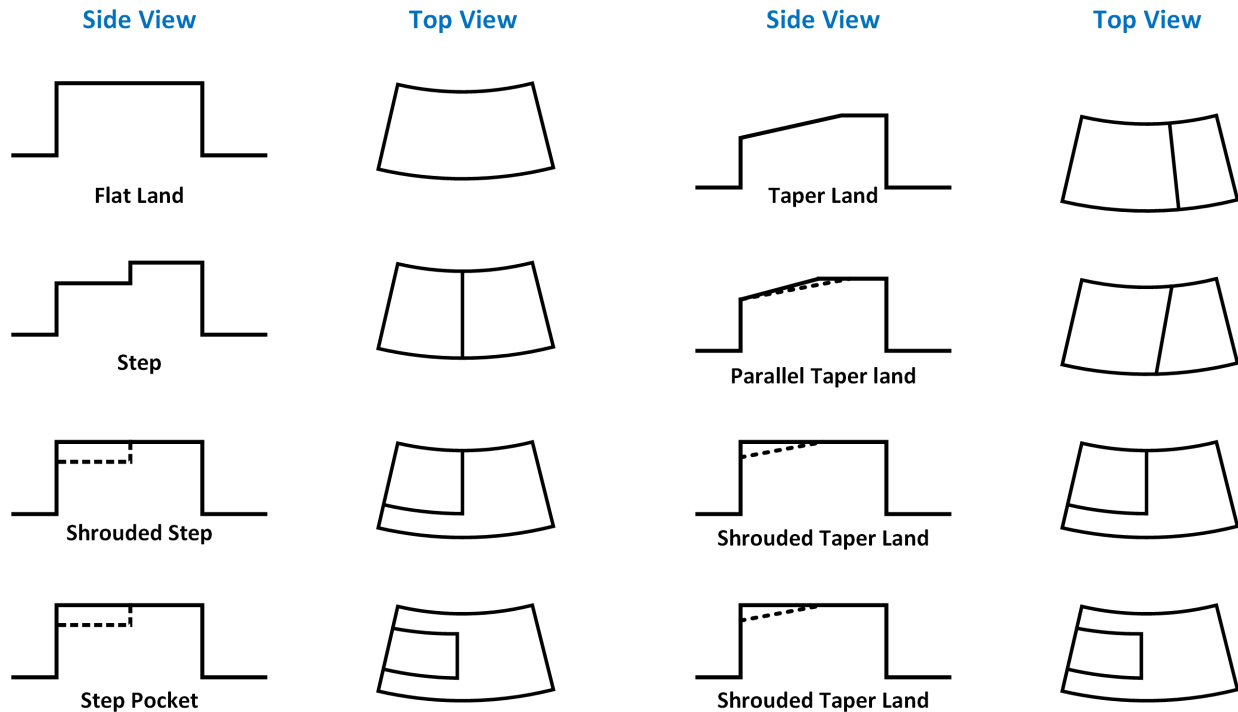

Figure 5: Flat land fixed geometry bearing

Figure 6: Fixed geometry bearing designs

To improve load capacity, a converging wedge needs to be added to the pad surface. Figure 6 shows a variety of ways to create a converging film on a fixed pad. Taper land and parallel taper land are relatively popular designs. In these designs, a converging taper is machined from the pad leading edge to somewhere near the trailing edge. While the taper is responsible for generating hydrodynamic pressure, the flat region near the trailing edge provides a surface to set the rotor float or position, as well as facilitates manufacturing. The shrouded taper land can be used when inadequate oil flow is a concern because the shroud or rail helps to keep the lubricant inside the clearance. Since the film shape has to be converging, all the designs in Figure 6, except the flat land, are unidirectional, which means they cannot support any significant load if the rotational direction is reversed.

The thrust collar and bearing surface should remain parallel so that all pads equally share the load. In addition, the axial runout of the thrust collar must be very small. However, When shaft angular misalignment is present, some pads will be more heavily loaded than the other. With exceedingly high load, one pad can fail due to high temperature or rub. This creates a chain reaction as the loads on the remaining pads will increase due to the loss of the first pad, quickly leading to the bearing failure. Fixed geometry bearings, and tilting pad bearings by themselves, do not have the capability to compensate for this misalignment. Another limitation is that the bearing surface, such as the taper slope, can be optimized only for a single operating point of speed/load combination.

A tilting pad bearing is shown in Figure 7. A tilting pad bearing can incorporate self-equalizing links to handle the misalignment between the bearing and the thrust collar. As shown in Figure 8, in this popular design, the pads sit on the upper level link and the lower level link sits on the retainer base. With misalignment, the pads that would be heavily loaded will be pushed down. Consequently, the link will push up the pads on the opposite side, keeping the bearing surface parallel to the thrust collar surface. It should be pointed out that the self-equalizing link is used to handle *static* misalignment from machining imperfections in the bearing and casing structure. It cannot be applied to compensate dynamic motion due to the thrust collar axial runout.

The American Petroleum Institute (API) requires the use of the self-equalized tilting pad design in some machines. Table 1 summarizes the requirements from various API specifications.
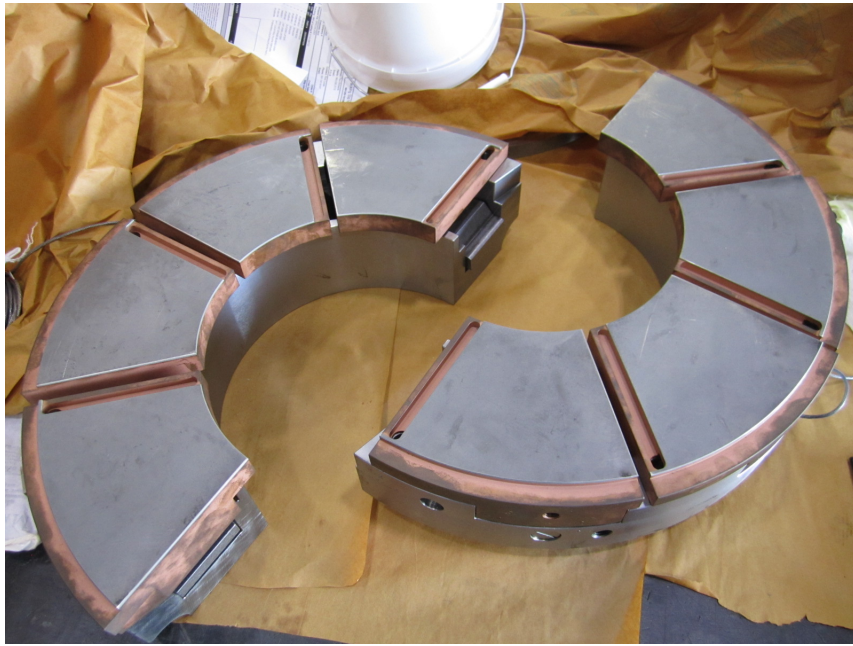
Figure 7: Tilting pad thrust bearing

Table 1: Machines requiring self-equalizing thrust bearings

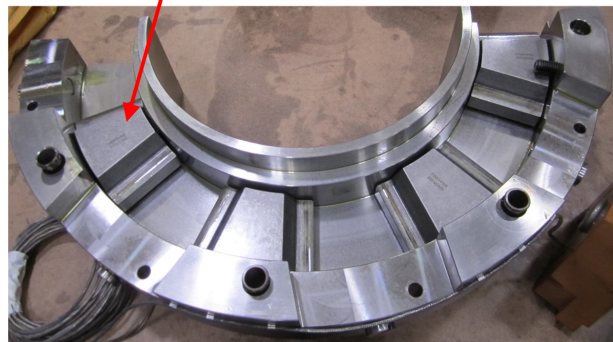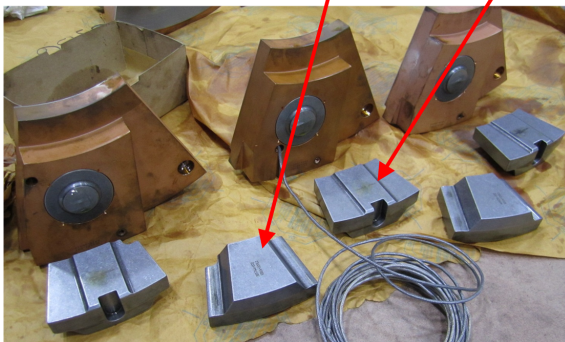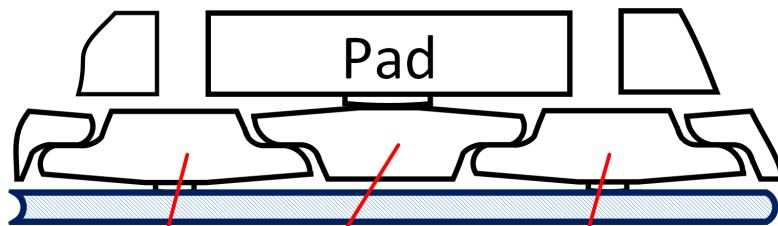| API standard	Machinery type	Required?
610	Centrifugal pumps	Yes
612	Steam turbines	Yes
616	Gas turbines	Yes
617 Part 1	Beam compressors	Yes
617 Part 2	Integrally geared compressors	No
617 Part 3	Expander – compressors	No

Figure 8: Tilting pad thrust bearing with self equalizing link

Hydrodynamic Pressure and Load Capacity

The load carrying capacity comes from the hydrodynamic pressure generated in the converging thin film. The film thickness and shape are dictated by design and operating parameters. For example, the film thickness will decrease with increasing load or decreasing speed. The design parameters influence the performance by controlling, or tuning, the converging film shape. For a tilting pad bearing, the amount of circumferential pivot offset has the most significant influence on load capacity.

Because of its symmetry, central pivot bearings ($\phi_c = 0.5$) must be used in applications where reverse rotation with appreciable load is expected. Similar to the flat land fixed pad, a central pivot tilting pad cannot develop hydrodynamic pressure according to the classic lubrication theory (isoviscous film, rigid pad and collar). One may argue that the pad can tilt to create a converging film. However, in steady state equilibrium, the pressure must be balanced such that the moment about the pivot is zero. The classic lubrication theory would predict no such equilibrium position can exist. In reality, the pad is experiencing elastic deformation in operation. Supported by a pivot on its back, the hydrodynamic pressure effectively produces a crown on the pad surface, as illustrated in Figure 9. Moreover, the pad is hotter on the film surface than the back surface because the heat source is viscous shearing in the film. Therefore, thermal deformation causes it to "warp", further increasing the effective crown and providing the necessary convergence for generating hydrodynamic pressure.

Since its load capacity is highly dependent on deformation, a central pivot bearing is usually sensitive to design details, such as pad thickness, cutouts and pivot design. A crown can be manufactured on the surface to improve load capacity. Raimondi investigated the relationship between crown and load capacity and found the optimum crown ratio to be 0.6. The crown ratio is the crown height divided by the minimum film thickness. For example, if the minimum film thickness is 25 μm, the crown should be $0.6 \times 25 = 15$ μm to produce the highest load capacity (Ball (1996)). However, a crown is usually difficult to manufacture and could be worn out in applications that require frequent start/stop.
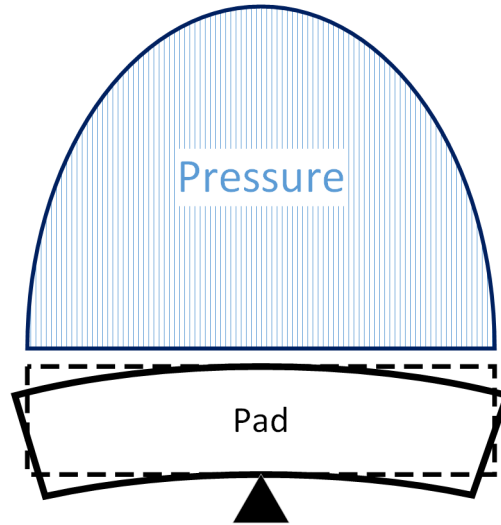

Figure 9: Deformation of a tilting pad under pressure load

Figure 10(a) compares the resulting pad tilt angle under operation for various amounts of pivot offsets based on theoretical predictions. The pad has a 254 mm (10 in) outer diameter and a point contact pivot of 0.5 radial offset. The rotational speed is 7000 rpm and the load is 2.07 MPa (300 psi). ISO VG32 oil is supplied at 49 °C (120 °F). As shown in this figure, the pad has increasing tilt angle with increasing offset, which means the film becomes more converging as the pivot is moved towards the trailing edge. The increase of tilt angle is necessary to maintain zero moment about the pivot to achieve steady state equilibrium. Recalling that a converging clearance is one of the three ingredients to produce hydrodynamic pressure, one should expect that a higher offset leads to higher load capacity.

As shown in Figure 10(b), the film thickness indeed increases with increasing offset. The blue line plots the film thickness at the pivot location, which can be regarded as the averaged film thickness. The red line represents the minimum film thickness that typically occurs at the trailing edge. Figure 10(b) shows that the film thickness *on average* is substantially increased with increasing offset. However, due to more clearance closure at the trailing edge, the minimum film thickness has noticeably less improvement in the high offset design. As indicated in Figure 10(b), further increasing offset will start to decrease the minimum film thickness and increase the maximum local pressure (see Figure 10(c)). Therefore, the circumferential offset typically ranges from 0.5 to 0.65 in industrial applications. Comparing the pressure contours in Figure 11, higher pivot offset also shifts the pressure peak towards the pad trailing edge.

The radial offset can also be used to fine tune the bearing performance. The typical range for radial offset is from 0.5 (center) to 0.55 (shifted towards outer diameter). The film near the outer diameter tends to produce higher pressure due to
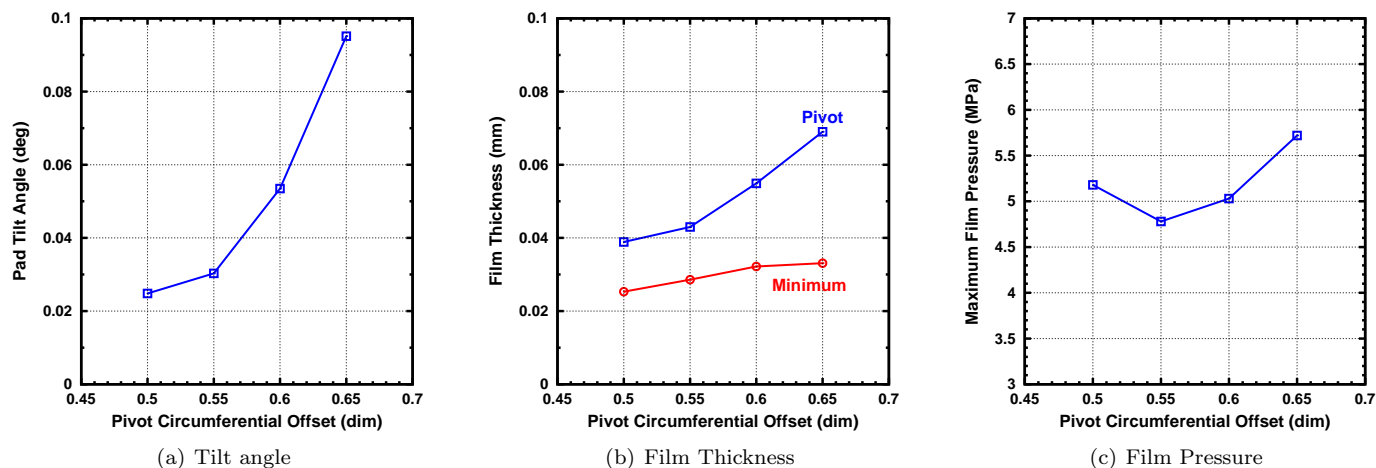
(a) Tilt angle   (b) Film Thickness   (c) Film Pressure

Figure 10: Influences of circumferential pivot offset
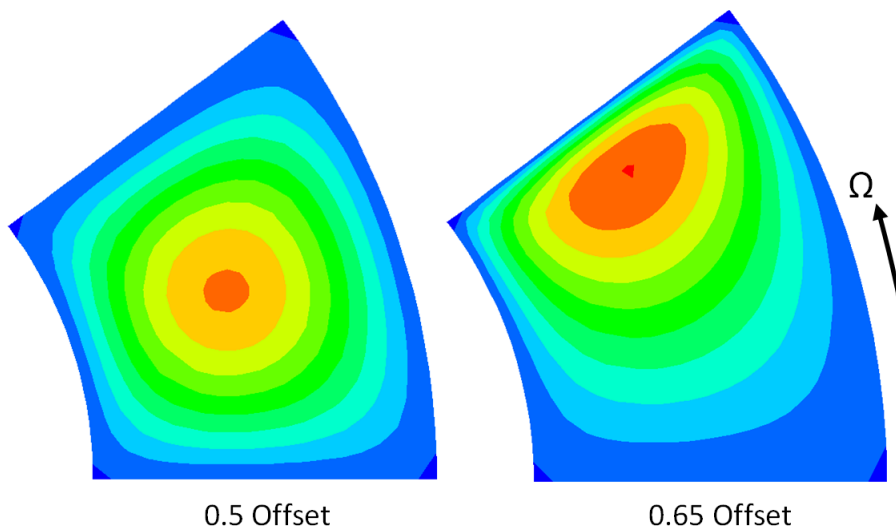

0.5 Offset   0.65 Offset

Figure 11: Pressure contours, 0.5 circumferential offset versus 0.65 circumferential offset

the higher surface velocity ($U = \Omega R$). Therefore, with 0.5 radial offset, the pad tilts outward, resulting in higher clearance at the outer diameter. Increasing radial offset causes the pad to tilt inward, adjusting the radial film thickness distribution, and thus, affecting the hydrodynamic pressure.

Load capacity is also influenced by the pivot design. Schematically shown in Figure 12, the line contact pivot is often used in high load applications in order to minimize the radial "unwrapping" from elastic deformation. With a point contact pivot, the hydrodynamic pressure causes the pad to unwrap in both circumferential and radial directions. While the circumferential unwrapping can be very beneficial (the resulting crown gives a central pivot bearing load capacity), the radial unwrapping increases the clearance near the inner and outer edges and reduces the load capacity. A line pivot diminishes the radial unwrapping by enhancing its rigidity. However, when heavily loaded, the thrust collar also deflects more at its outer diameter. Unlike a point pivot pad, a pad with line pivot cannot tilt radially to compensate such collar deformation. Another option is the ball and socket design. This type of pivot has surface contact, and thus, is more rigid than point contact yet allows radial tilt motion.

Some API specifications require the operating load be no more than 50% of the bearing's *ultimate load rating*. The idea is straightforward: since high load leads to bearing failure, it should be limited with a comfortable margin for safe operation. For example, in API 617, the ultimate load rating is defined as "load that shall produce the minimum acceptable oil film thickness without inducing failure during continuous service, or the load that shall not exceed the creep initiation or yield strength of the babbitt or bearing material at the location of maximum temperature on the pad, whichever load is less." (API 617 (8th Edition))

There are several reasons for this large factor of safety:

1. The requirement was introduced many years ago, before accurate analysis tools were available. Thrust bearing sizing was largely based on interpolation and extrapolation from available test data. This required a large factor of safety.

2. Knowledge of the applied thrust load, even to this day, has a high uncertainty.

3. Thrust bearings must be designed to accommodate off-design, transient conditions such as surge and system upsets that can result in larger than expected thrust loads as well as dynamic thrust loads (loading and unloading the thrust bearing). This requires significant additional margin to ensure a robust design.

4. Many other parameters that influence the thrust bearing are also subject to variability and uncertainty such as inlet oil flow, inlet oil temperature, thrust collar runout, and misalignment.

Although the ability to analytically predict the performance of a thrust bearing has improved tremendously, many of the other factors that led to the large factor of safety remain. The authors recommend careful consideration before violating this API requirement.
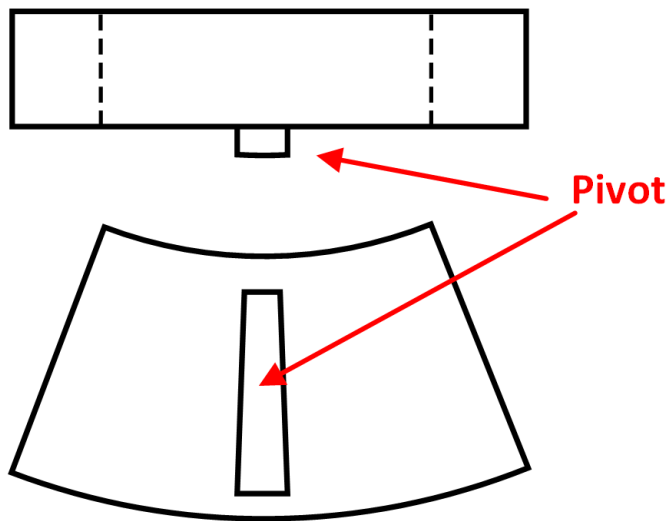

Figure 12: Schematics of line pivot tilting pad

Viscous Shearing and Temperature Rise

As shown in Figure 4, the lubricant is stationary on the pad surface and has the velocity of U on the thrust collar surface, per the standard, no-slip boundary condition in fluid mechanics. This non-uniform velocity leads to friction between the fluid particles, generating heat and causing temperature rise. The intensity of this internal friction is signified by the shear stress $\tau = \mu \left(\partial u / \partial y \right)$. Assuming laminar shear flow, the velocity profile is linear and its gradient across the thin film is $\partial u / \partial y = U / h$. Therefore, the shear stress can be approximately calculated as $\tau = \mu \left(U / h \right)$. From this equation, it is clear that more intense viscous shearing, and thus heat generation, can be produced by either higher viscosity (μ), higher surface velocity (U), or smaller film thickness (h).

The resulting thermal effects have significant influence on a thrust bearing's performance. First, oil viscosity typically undergoes exponential reduction with temperature rise. Second, the thermal deformation changes the operating film shape, especially the effective crown for a central pivot pad. In addition, the maximum pad temperature is an important operational parameter that indicates the bearing's health. The temperature limit for a Babbitt bearing is about 130 °C (265 °F), above which the Babbitt may start to creep under pressure load.

Figure 13 shows the temperature distributions on the same thrust pad with 0.5 and 0.65 circumferential pivot offsets. Pad temperature increases from the leading edge to the trailing edge as the result of continuous internal viscous shearing along the flow path. The temperature is higher near the outer diameter because of the higher local surface velocity. Similar to the pressure, the maximum temperature location is shifted closer to the trailing edge with the 0.65 offset pivot.

The health of a thrust bearing is typically monitored by temperature sensors within the loaded pads. Per API 670 (4th Edition), the temperature sensor should be placed at 75% of the pad width radially from the inner diameter, and at 75% of the pad length from the leading edge. However, the sensor does not measure the actual maximum temperature in reality. As shown in Figure 13, the maximum temperature is not at the 75/75 location, but closer to the trailing edge, especially in case of the 0.65 pivot offset. Also note that the sensor is not on the Babbitt surface, but imbedded in the base metal and at

least 0.8 mm (0.03 in) below the Babbitt bond line. Since the measurement is always lower than the actual maximum, the temperature limits based on the measurement must be set below the value of failure concern.
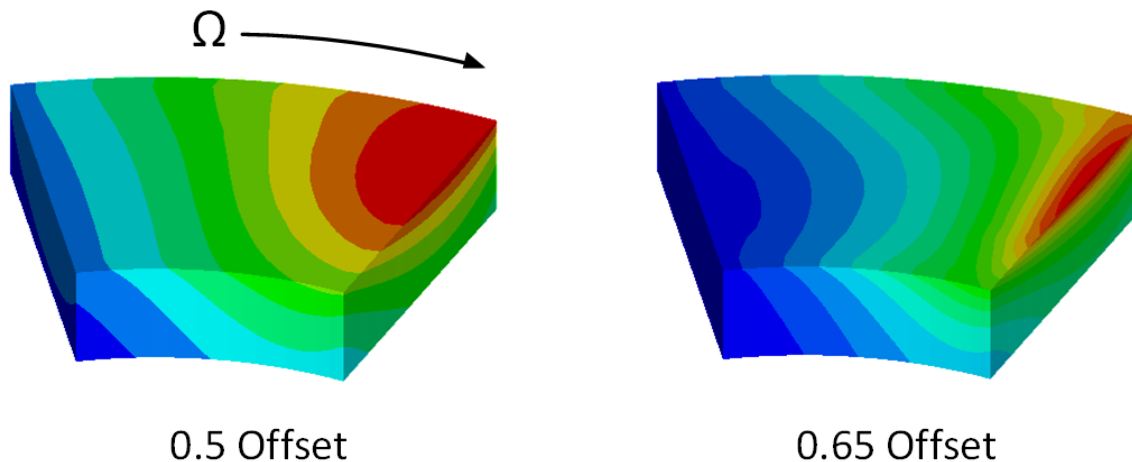

Figure 13: Pad temperature contours, 0.5 offset versus 0.65 offset

The mechanical strength of Babbitt decreases at elevated temperature. For example, Grade 2 Babbitt has yield strength of 42 MPa at 20 °C, which reduces to approximately half of this value at 100 °C. Therefore, the weak location on a pad is where both the pressure and temperature are high. In case of the 0.65 circumferential offset, although the sensor at 75/75 location does not capture the maximum temperature, it is still likely monitoring the weakest location since the local pressure is high. Babbitt creep is a likely failure mode for high speed bearings. To assess the risk, the yield strength of Babbitt on the pad surface can be plotted based on the temperature distribution. Superimposing the pressure distribution, it is easy to identify the location that has the lowest safety margin against local creep.

Pad temperature is dictated by both operational and design parameters. To demonstrate the influence of various parameters, the same 254 mm (10 in) bearing is used here again. The pivot circumferential offset is 0.6 and the sensor is assumed to be 2.54 mm (0.1 in) below the Babbitt surface. Keeping the load constant at 2.07 MPa (300 psi), Figure 14(a) shows that the temperature varies with speed, and the 75/75 measurement is consistently below the actual maximum. However, it also shows that the temperature does not monotonically increase with increasing speed, as one might intuitively anticipate. Instead, a notable dip can be observed between 10000 rpm and 14000 rpm. This temperature decrease is the result of flow regime transition from laminar to turbulent, which has been experimentally confirmed in both thrust bearings (Capitao *et al.* (1976), Mikula (1985), Mikula (1986)) and journal bearings (Suganami & Szeri (1979), Simmons & Dixon (1994)).

Figure 14(b) shows the maximum pad temperature as a function of load while the speed is kept constant at 7000 rpm. From this figure, it can be concluded that one way to lower the operating temperature is to reduce the specific load. This can be achieved by reducing the inner diameter, maximizing the arc length, and increasing the outer diameter. Increasing outer diameter implies that a larger bearing is required to carry the load. However, the benefit of increasing the outer diameter is limited because larger diameter means higher surface velocity, and thus, more intense viscous shearing. Beyond a certain threshold, the effect of high surface velocity overwhelms the unit load reduction, leading to higher temperature.

Among the various design parameters, the circumferential pivot offset has strong influence on pad temperature. Figure 14(c) shows the maximum pad temperature as the function of pivot offset. With a central pivot, the pad temperature is fairly high at 116 °C. The temperature shows monotonic and substantial decrease as the pivot is moved towards the trailing edge. The maximum temperature is lowered by 30 °C when the offset is increased to 0.65. A similar level of reduction was reported by Gardner (1988).

Improved load capacity is one of the reasons why the offset bearing operates at lower temperature. As shown in Figure 10(b), the high circumferential offset leads to increased film thickness. Since $\tau \approx \mu(U/h)$, the viscous shearing is reduced as the result of increased h. The lower temperature is also the result of a more converging film shape. Figure 15 schematically shows the oil flow between two pads. Lubricant entering a pad (Q_{in}) is composed of two streams: oil leaving the trailing edge of the upstream pad (Q_{out}) and oil from outside (Q_{supply}). The oil from the previous pad is relatively hot due to internal viscous shearing on that pad, and is called *hot oil carryover*. The oil from outside is relatively cool. To achieve low oil inlet temperature, the hot oil carryover should be minimized while the cool supply oil should by maximized. With a large tilt angle, the trailing edge has a small film thickness, which helps to scrape or block the hot oil carryover. Meanwhile, the film thickness at the leading edge is large, allowing the entry of more cool external oil. The combined effect is that the inlet

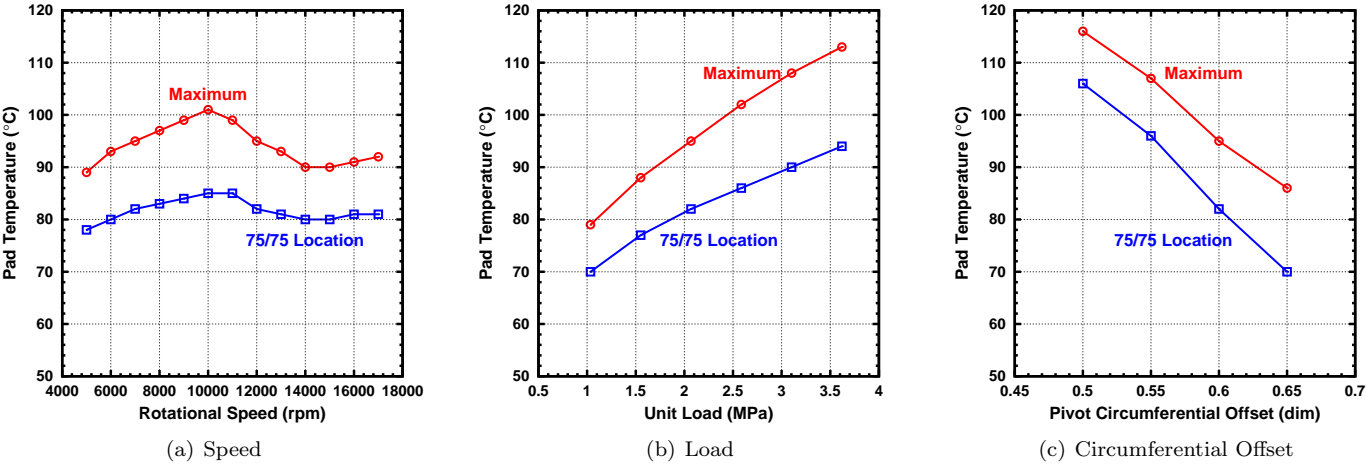(a) Speed   (b) Load   (c) Circumferential Offset

Figure 14: Influences on pad temperature

oil has the increased percentage of the cool oil. Therefore, with high offset pivot, oil enters the pad leading edge at a low temperature and is heated up at a relatively low rate; the end result is a significantly reduced maximum temperature near the trailing edge. One unfortunate aspect is that the offset bearing requires more oil flow to fill the space.

Another effective way to reduce the operating temperature is to use copper pads. Taking advantage of copper's high thermal conductivity, switching the pad material from steel to chrome copper will typically reduce the pad temperature by 10 to 15 °C (Gardner (1988)). This approach is especially attractive in applications where the use of offset pivots is not allowed due to reverse rotation or other limitations. Other measures to reduce temperature involve using an evacuated housing and/or direct lubrication designs, which will be discussed in the next section.
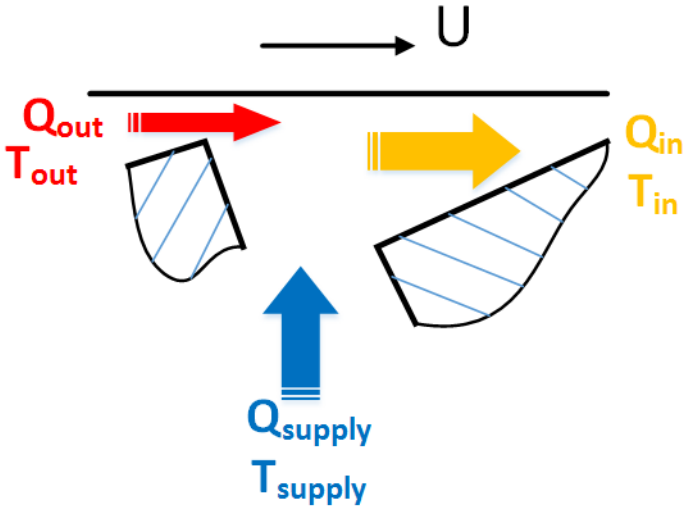

Figure 15: Groove mixing between two pads

Oil Flow, Power Loss and Direct Lubrication

Figure 16 shows the velocity vectors on the axial midplane of a pad, halfway through the film thickness. The velocity is largely circumferential as the result of the collar's shear drag. The circumferential velocity produces the inlet flow at the leading edge and the hot oil carryover at the trailing edge. Meanwhile, the velocity vectors also have radial components that cause the leakage on the inner and outer diameters. Due to centrifugal pumping effect, the ID leakage usually cannot flow out of the bearing through the inner bore clearance. Therefore, the net flow leaving the bearing is basically the OD leakage since both the hot oil carryover and ID leakage are internally circulated.
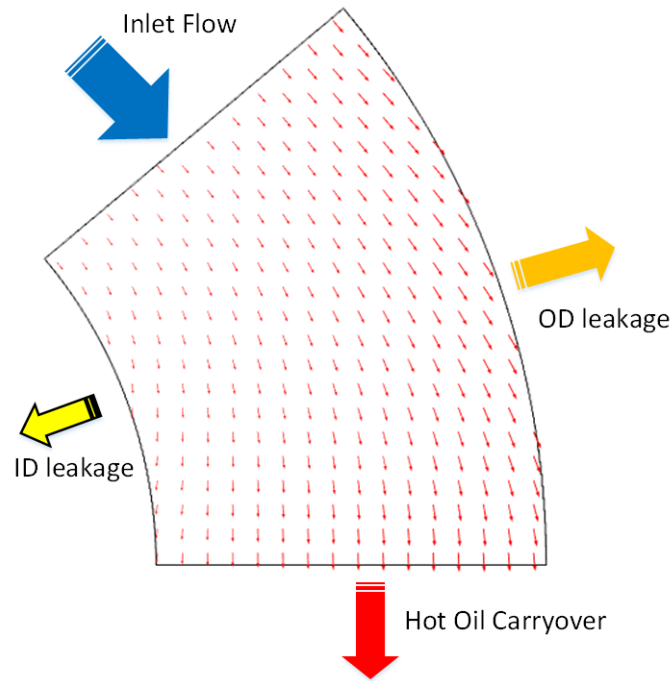
Figure 16: Velocity field on the axial mid-plane and oil flow across edges

How the oil flows within the housing is crucial to a bearing's thermal performance. Figure 17 shows the oil flow in a conventional flooded housing. In this design, oil is supplied into the bearing through radial holes behind the pads. After reaching the inside bearing bore, it is distributed circumferentially by the rotating shaft, mixed with the ID leakage and feeds the radial grooves between pads. The exit flow is eventually collected by a tangentially oriented drain hole on top.
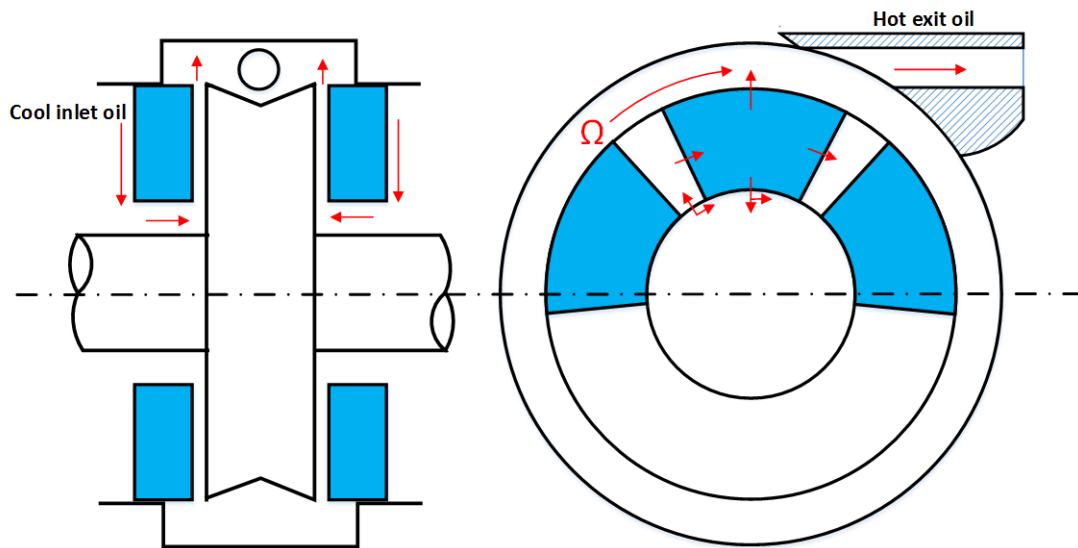

Figure 17: Oil flow in a conventional flooded housing

Since the only exit is on top, the design in Figure 17 essentially creates an oil bath or reservoir in which the pads are submerged. Consequently, this type of housing and operation are referred as "flooded". Since the pads are always lubricated, the purpose of supplying oil is to carry away the heat generated by viscous shearing and keep the oil bath reasonably cool. For example, API 612 (6th Edition) requires that the oil temperature rise through the bearing and housing shall not exceed 30 °C (50 °F).

High temperature is a potential problem for flooded operation because the hot oil is not immediately drained out of the bearing cavity. Another disadvantage is the parasitic power loss produced by the collar being submerged and churning in

oil. From the energy standpoint, the viscous shearing converts mechanical power into heat. This parasitic churning loss, which can be quite high at high speeds, further heats up the oil surrounding the pads. To keep the oil bath acceptably cool, the supply flow rate could well exceed the necessary amount to lubricate the pads, leading to excessive oil consumption in addition to high power loss.

The evacuated housing provides an alternative to address this problem. As illustrated in Figure 18, the drain hole is located on the bottom, eliminating the oil bath and the resulting parasitic churning loss. In addition to improved efficiency, it reduces operating temperature because the pads are no longer surrounded by hot sump oil. Since there is no oil bath, the oil leaving the bearing must be replenished by fresh oil from the lube supply system. Therefore, the minimum oil supply should equal the leakage across the outer diameter, which is dictated by speed, load and the bearing design.

The risk of evacuated operation is starvation due to insufficient oil flow to the pads. A pad is starved if there is not enough oil to fill the pad's inlet clearance ($Q_{out} + Q_{supply} < Q_{in}$ in Figure 15). When starved, a pad has a reduced surface area to carry the load, resulting in smaller film thickness, higher temperature and less power loss. In other words, the bearing effectively becomes smaller (Artiles & Heshmat (1987)). Gardner (1998) tested the influence of oil flow rate on temperature and power loss. As the oil flow decreased from a relatively high level, both temperature and power loss initially showed little change; however, past a certain threshold, temperature started to rise significantly, which is accompanied by substantial power loss reduction. This is due to the fact that, initially, there was adequate oil to lubricate the pads ($Q_{out} + Q_{supply} \geq Q_{in}$) even though the flow rate was decreasing. In this stage, the redundant oil simply bypassed the pad clearance, and thus, had little influence on the bearing's performance. However, further flow reduction eventually led to starvation. In field operation, starvation is sometimes detected as abnormally high pad temperature.
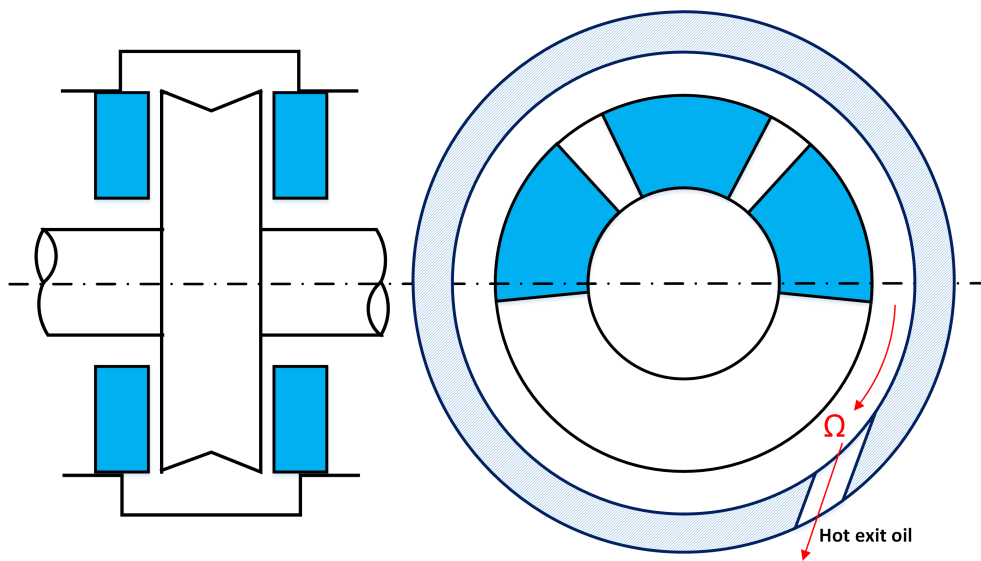

Figure 18: Schematics of an evacuated housing

To ensure oil reaches the pad surface, evacuated housings are often combined with the use of directly lubricated bearings. One type of such design is to machine or attach an oil feeding groove to the pad leading edge; oil is directly supplied into this groove. The other type is to install a bar with nozzles in front of the pad; oil is sprayed out of the nozzles. Figure 19 shows the examples of those two types of designs. Utilizing the same idea, many variants have been developed by different bearing manufacturers. Performance of the evacuated direct lube bearings were experimentally studied and discussed by Stewart (1999).

Directly lubricated bearings require less oil since bypass leakage, i.e., supply oil that never reaches the pad, is minimized. In theory, the oil supply flow rate should be at least as much as the OD leakage of the entire bearing. In reality, some extra margin is usually required to cover various uncertainties. For example, Gardner (1998) suggested that a multiplier of about 1.5 be applied for the specific design tested in his work. Directly lubricated bearings can also be used in flooded operation if the power loss is not a concern. Since cool oil is directly sent to the pad inlet, which presumably reduces the hot oil carryover, the operating pad temperature is still noticeable lower than that in a comparable conventional bearing (Mikula (1988)).

Directly lubricated bearings can experience damage in the event that oil supply flow is interrupted. It is recommended that the use of direct lube bearings be accompanied by emergency lubrication systems such as an overhead rundown tank or pressurized accumulator.
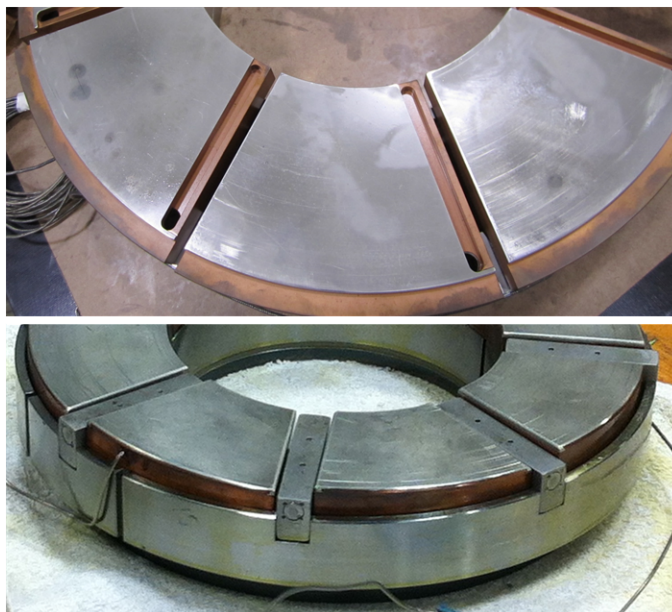
Figure 19: Examples of direct lubrication bearings

Dynamics

Steady-state operation implies that the bearing force balances the *static* axial load and the system is in equilibrium. In reality, there are also some *dynamic* forces acting on the rotor, causing vibration. For example, if the thrust collar is perturbed towards the bearing, the hydrodynamic force from the bearing will increase to counteract the collar's axial motion. In a linear system, the dynamic bearing force is assumed to be proportional to the collar's displacement and velocity. For axial translational motion,

$$-F_z = K_{zz}z + C_{zz}\dot{z}$$

where K_{zz} is the stiffness coefficient and C_{zz} is the damping coefficient. This equation means, when the thrust collar is vibrating, the reacting bearing force is proportional to both the vibration amplitude (z) and velocity ($\dot{z}$).

The equation above defines the axial force as the result of the collar's axial translation. The dynamic motion could also involve one side of the thrust collar approaching the bearing. Consequently, the bearing will generate a resistive moment against such tilt motion. Therefore, a thrust bearing's dynamic coefficients also involve the moments and angular displacements. For a journal bearing, the journal has two degrees of freedom (translation in x and y) relative to the bearing, therefore, the dynamic coefficient (K or C) are represented by 2×2 matrices (He *et al.* (2016)). For a thrust bearing, its dynamic matrices are 3×3 since the collar has three degrees of freedom (translation in z and tilting about axes x and y).

Similar to the journal bearing, if a thrust bearing has tilting pads, its dynamic coefficients are also dependent on the vibration frequency. This frequency dependency should not be confused with the dependency on the rotational speed. The bearing dynamics are definitely dependent on the shaft rotational speed, as surface velocity is one of the three ingredients for hydrodynamic pressure. However, even when the speed is constant, the dynamic coefficients are different for different vibration frequencies. This characteristics is due to the fact that a tilting pad bearing constitutes a high order dynamic system.

Unlike journal bearings, the thrust bearing generally does *not* have significant influence on a machine's rotordynamics. Rodriguez (2000) included the thrust bearing dynamics in the analysis of several machines including centrifugal compressors, a steam turbine, a gas turbine and a hot gas expander. He found that the thrust bearing could be influential if the mode shape had considerable slope at the bearing location; and the inclusion of thrust bearing dynamics affected the predicted rotor stability and unbalance response. Nevertheless, it is typical not to include the thrust bearing in a lateral rotordynamic analysis.

However, the thrust bearing dynamics could be vitally important in two situations. First, if the system has a helical gear, and thus, the lateral, torsional and axial vibrations are all coupled together. Second, the machine is experiencing axial vibration. DeCamillo (2014) investigated the subsynchronous axial vibrations under no or low load conditions on a test rig. No or low load condition occurs during a machine's no load spin test or thrust load reversal. As shown in this study, a distinctive subsynchronous vibration was observed. This axial vibration, which is also mentioned in Ball (1996), appears to be related to some resonance. When unloaded, there is also a very low frequency signal in the vibration spectrum. This very

low frequency signal is caused by the random shifts in the shaft position between the active and slack bearings. The common methods to mitigate the subsynchronous axial vibration are also discussed in DeCamillo (2014).

Interaction of Operational Aspects

The interaction of various operational aspects are summarized in Figure 20. On top, we have the three necessary ingredients to generate hydrodynamic pressure in steady state. Due to the hydrodynamic pressure, the pad and collar experience mechanical deformations, which in turn change the shape of the converging wedge. Meanwhile, those three ingredients also lead to internal viscous shearing that generates heat and causes the temperature rise. The temperature rise has two consequences: viscosity reduction of the lubricant and thermal deformations of the pad and collar. The viscosity reduction changes the lubricant and the thermal deformations change the wedge shape. The other consequence of the viscous shearing is the friction power loss. The power loss and temperature rise are related because, from the energy standpoint, the consumed mechanical power is converted into heat, leading to the temperature rise.
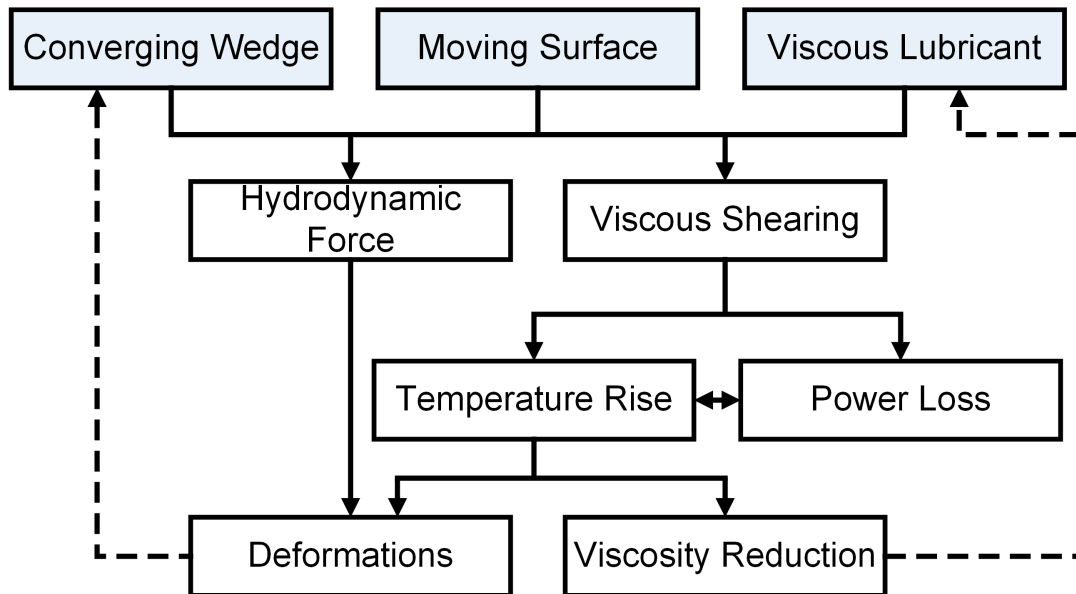

Figure 20: Interaction of operational aspects, He *et al.* (2016)

MODELING ASPECTS

Knowing the thrust bearing's performance is critical for a machine's overall reliability. While testing is very useful, the bearing may not be available for testing in its design stage. Even if it is available, it may not be possible to test all operating conditions, and/or accurately measure the performance parameters of interest. In practice, its performance is often theoretically predicted by some computer software. To ensure proper use of the software, it is important to understand what the computer actually does behind the user interface. This section presents the theoretical models that are typically used in thrust bearing analysis.

A typical thrust bearing analysis only models a single pad, basically assuming no misalignment and all pads function identically. The global performance parameters, such as the power loss, total oil flow and dynamic coefficients, are obtained by assembling all pads together.

Hydrodynamic Pressure

As the source of load carrying capacity, hydrodynamic pressure is the center of the bearing analysis. In general fluid dynamics, the flow field has four unknowns: three velocity components (u, v, w) and pressure (p), assuming laminar flow. Those variables are obtained by solving the three momentum equations coupled with the continuity equation. This is not a trivial effort.

For a bearing analysis, fortunately, it is not necessary to solve those nonlinear equations because the lubricant film is very thin (the h/D is on the order of 10^{-3}). The thin film assumption enables *dramatic* simplifications of the momentum equations, primary by ignoring the fluid inertia. Consequently, the velocity components in the circumferential and radial

directions can be solved from the simplified momentum equations. Substituting the velocities into the continuity equation and integrating across the thin film, the governing equation for the hydrodynamic pressure is obtained.

$$\frac{\partial}{\partial x}\left(\frac{h^3}{12\mu}\frac{\partial p}{\partial x}\right) + \frac{\partial}{\partial z}\left(\frac{h^3}{12\mu}\frac{\partial p}{\partial z}\right) = \frac{U}{2}\frac{\partial h}{\partial x} \tag{2}$$

Equation 2 is the classic Reynolds equation which assumes constant viscosity across the thin film and laminar flow. From this equation, we can identify the three ingredients for hydrodynamic pressure: the fluid must be viscous ($\mu \neq 0$); there must be relative motion ($U \neq 0$), and the clearance must be converging ($\partial h/\partial x < 0$). The boundary condition is that the pressure equals some known ambient pressure on the boundary. One example of the pressure solution is shown in Figure 21. This is the same 0.5 circumferential offset bearing whose two dimensional pressure contours are presented in Figure 11. Note that the Reynolds equation is two dimensional. Constant across the thin film, the pressure distribution is solved in the circumferential and radial directions.
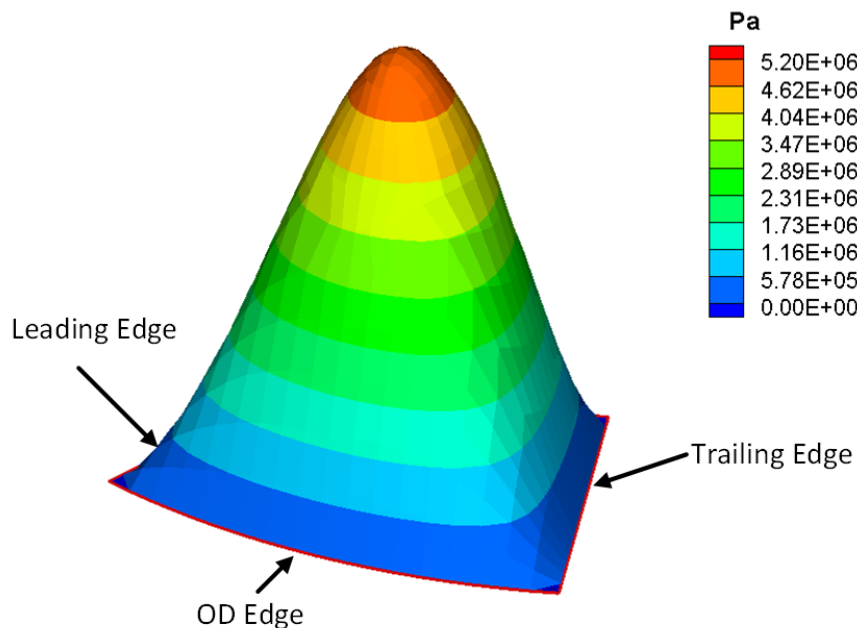

Figure 21: Pressure solution from the Reynolds equation

If a tilting pad is heavily loaded or crowned, the film shape could be diverging near the trailing edge as the result of the circumferential unwrapping (see Figure 9). Applying the boundary condition above, the Reynolds equation will give a negative solution in the diverging clearance region. Physically, this negative pressure tries to draw the fluid from the surroundings. If the bearing is submerged in high pressure fluid, such as in a canned motor pump, fluid will indeed be drawn into the diverging clearance across the inner and outer diameters; and the pressure will be negative *relative to* the high ambient pressure. However, in most applications, the film will cavitate since there is no high pressure fluid surrounding the pads. Instead, the film ruptures and two phase flow is developed. Consequently, the nonphysical negative solution from the Reynolds equation must be corrected. In other words, the cavitation boundary condition must be applied by setting the pressure in the cavitation region at some constant cavitation pressure.

The classic Reynolds equation was later extended to allow variable viscosity across the thin film and turbulent flow. The centrifugal body force can also be included in the lubricant film for the thrust bearing (Pinkus & Lund (1981), Brockett (1994)). As pointed out by Pinkus & Lund (1981), the centrifugal body force tends to reduce the load capacity, and thus, should be included in the Reynolds equation. In the authors' experience, the solution without centrifugal force generally gives satisfactory predictions, suggesting that its effect is likely secondary compared to the thermal and elastic effects.

Temperature

The film temperature is governed by the three dimensional energy equation below.

$$
\underbrace{\rho C_p \left(u\frac{\partial T}{\partial x} + v\frac{\partial T}{\partial y} + w\frac{\partial T}{\partial z} \right)}_{\text{Convection}} =
$$

$$
\underbrace{\frac{\partial}{\partial x}\left(k\frac{\partial T}{\partial x}\right) + \frac{\partial}{\partial y}\left(k\frac{\partial T}{\partial y}\right) + \frac{\partial}{\partial z}\left(k\frac{\partial T}{\partial z}\right)}_{\text{Conduction}} + \underbrace{\mu\left[\left(\frac{\partial u}{\partial y}\right)^2 + \left(\frac{\partial w}{\partial y}\right)^2\right]}_{\text{Heat Generation}} \tag{3}
$$

Similar to the Reynolds equation, Equation 3 is simplified from its general form using the thin film assumption. However, unlike the pressure, the temperature is not constant across the thin film and its distribution is three dimensional. The first order terms on the left hand side of the equation is the heat convection; the second order terms on the right hand side represent the heat conduction; and the last term is heat generation. The energy equation states the conservation of energy in the oil film: heat is generated due to internal viscous shearing; while some of this heat is conducted away across the film-solid interfaces, the majority of it is carried away by the flowing lubricant through convection.

The most important boundary condition for the energy equation is the inlet temperature at the leading edge because it establishes the basis from which the temperature will rise along the flow path. As discussed in Figure 15, the inlet oil is the mixture of the external oil and the hot oil carryover. The physics inside the groove is very complex involving mixing of fluid particles as well as heat transfer. The level of complexity is further exacerbated if direct lubrication features, such as the spray nozzles, are present in the model. The study of the groove mixing is still an ongoing research and computational fluid dynamics (CFD) provides a valuable tool as demonstrated by Ball (1996) and Grzegorz & Michal (2007).

In practice, most bearing analysis employ some simple model based on energy conservation in the groove (Ettles (1969), Heshmat & Pinkus (1986), Dmochowski *et al.* (1992)). Unfortunately, those simple formulas rely on some empirical parameter to calibrate the prediction. For example, in order to use such a formula, it is often required to prescribe a parameter λ, called hot oil carryover factor. The hot oil carryover factor is the percentage of the hot oil (Q_{out} in Figure 15) entering the pad inlet. A value of zero means all hot oil is blocked and the inlet oil is solely from the outside supply. $\lambda = 100\%$ means all hot oil leaving the trailing edge of the pad enters the inlet of the downstream pad. The hot oil carryover factor is typically estimated between 70% to 100% based on experience. However, error in its estimate will lead directly to errors in the predictions of the maximum temperature and other performance parameters.

To solve the energy equation, we also need to specify the temperatures on the pad and collar surfaces as necessary boundary conditions, which creates a dilemma. Because the pad is heated by the lubricant film, its temperature is dictated by the film temperature. This dependency means that the heat transfer in the film and pad are physically coupled together. Numerical iterations are usually employed to achieve mutually agreeable temperatures in both components (physically, temperature and heat flux must be continuous across their interface). Similarly, the film temperature is coupled with the heat conduction in the thrust collar. Due to rotation, the temperature on the collar is constant in the circumferential direction. Therefore, the collar's heat conduction can be modeled as a two dimensional axisymmetric problem.

Figure 22 shows the temperature distribution in the film of the same 254 mm (10 in) sector pad with 0.5 circumferential pivot offset. The pad surface is on top and the inlet is on the left. From the inlet, film temperature increases along the flow path and reaches the maximum near the corner of the trailing edge and the outer diameter. Note that the maximum temperature is very close to the pad surface as opposed to the collar surface. Referring to the velocity profile in Figure 4, the velocity near the stationary pad surface is relatively low compared to that near the moving collar surface. Consequently, the local heat convection is relatively weak, leading to high temperature near the pad surface. Figure 22 also shows the three dimensional film shape with the axial dimension greatly exaggerated. The concavity on the top surface means convexity on the matching pad surface, indicating the effective crown produced by elastic deformation.

The corresponding pad temperature can be found in Figure 13, which was obtained by modeling the pad heat conduction. The pad was modeled as a single domain with uniform material properties of the base steel. It is typically acceptable to ignore the different properties of the Babbitt. However, the surface layer must be modeled separately if its thermal conductivity is drastically different. For example, the pad in Figure 23 has its surface layer made of PEEK whose thermal conductivity is approximately two orders of magnitude smaller than that of steel. Consequently, almost all temperature variations take place on the surface. The base steel is largely isothermal as it is effectively insulated from the lubricant film.

Although relatively time consuming, it is necessary to solve the three dimensional temperature to achieve good accuracy, especially for a central pivot pad. As previously discussed, a central pivot pad relies on the effective crown to generate load capacity. Therefore, it is critical to accurately model the deformations including the thermal deformation. This requires the pad temperature be accurately predicted in the first place. One common simplification is to assume an adiabatic film. It
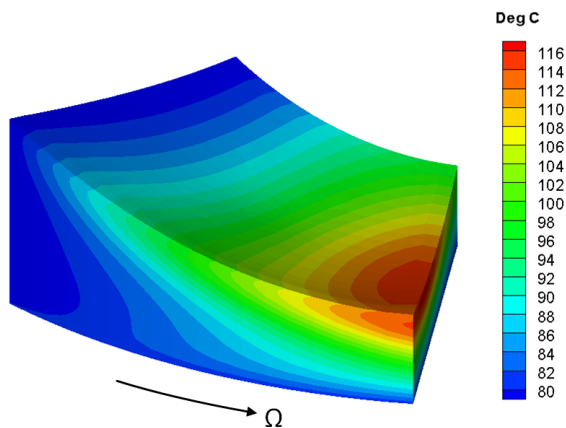
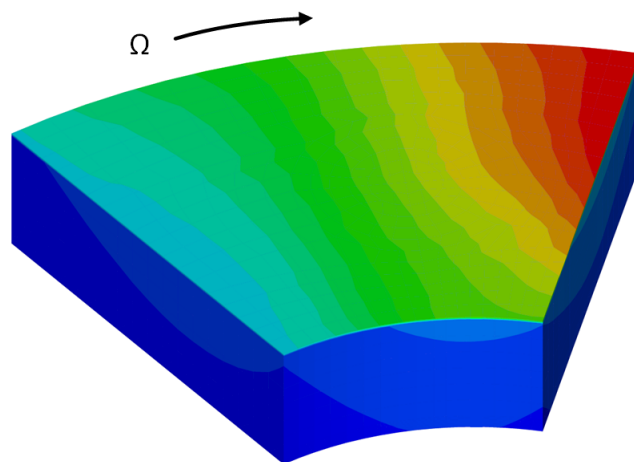Figure 22: Film temperature solution from the
energy equation

Figure 23: Temperature distribution on a pad
with polymer surface

should be pointed out that, besides inferior accuracy, the adiabatic assumption excludes the pad from the thermal analysis, and thus, is unable to model the pad thermal deformation.

Figure 24 plots the two dimensional axisymmetric temperature distribution on the thrust collar. The collar is clearly heated up by the active bearing while convection boundary condition is applied on the inactive or slack side.
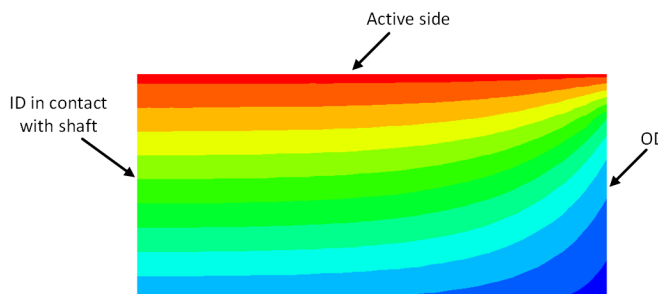

Figure 24: 2D axisymmetric temperature solution for the thrust collar

Elastic Deformation

Elastic deformation affects a bearing's performance by changing the shape of the converging wedge. It is absolutely necessary to model the elastic deformation for a 0.5 circumferential offset tilting pad or a flat land fixed pad. It is also highly recommended to include it in all tilting pad bearing analysis. A fixed pad usually has more rigid construction and an explicitly machined converging taper or step. Therefore, it might be acceptable to ignore the deformation if the operation condition is benign.

The three dimensional finite element method can be used to calculate the pad deformation. The advantage of the finite element method is its flexibility to model complex geometry. For a tilting pad, there could be cutouts near the leading and trailing edges, and/or on the back of the pad. Modeling those details is important if the bearing's performance is significantly influenced by how the pad deforms, such as one with a central pivot. Figure 25 shows the axial deformation of the 254 mm (10 in) sector pad with central pivot. The spherical crown is clearly shown by the blue circles (blue indicating negative displacement which is upward). The same crown is also shown in Figure 22 as the concave upper surface. Both mechanical and thermal deformations were included in the analysis.

Strictly speaking, the thrust collar also experiences three dimensional deformation. For example, the location of the maximum pressure is subject to more *local* mechanical deformation. However, the thrust collar is typically more rigid than a tilting pad, and its deformation is usually dominated by the *global* bending. Therefore, like its temperature, the collar's deformation is usually calculated using a two dimensional axisymmetric model. For the case in Figure 25, the corresponding axial deformation of the collar is shown in Figure 26. In this model, the inner diameter has fixed displacements and the hydrodynamic pressure is applied on the active side. The pressure must be circumferentially averaged since it is two dimensional. Blue color represents negative displacement, which is downward in Figure 26. The contours show the collar
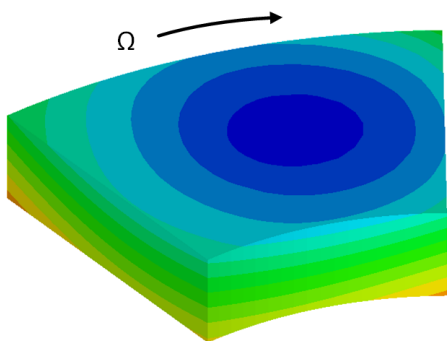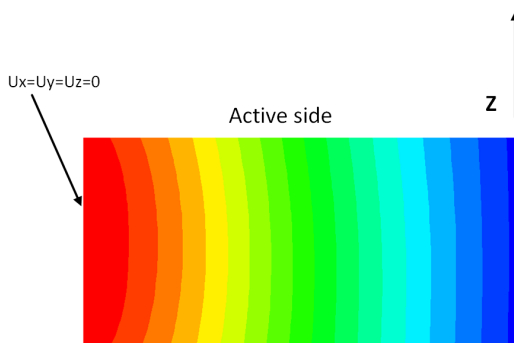
Figure 25: Pad axial deformation

Figure 26: Collar axial deformation

is bent away from the bearing. From the inner diameter, The deflection monotonically increases in the radial direction and reaches the maximum on the outer diameter.

Turbulence

At low speeds, the bearing flow remains in the laminar regime in which the flow is stable and the fluid particles move smoothly. The flow eventually becomes turbulent as the speed continues to increase. In turbulent flow, the fluid particles exhibit rapid and irregular fluctuation with time and position. Since they are constantly changing, it is impossible to track the instantaneous flow parameters such as velocity and pressure. Instead, the objective is to obtain their statistical mean values. The flow regime is dictated by the Reynolds number $Re = \rho U h / \mu$. The flow remains laminar if the actual Reynolds number is below a certain critical value. Above this critical Reynolds number, the flow becomes unstable and starts to transition into turbulence. It is developed into full turbulence when the Reynolds number surpasses a second threshold. From the definition of the Reynolds number, it can be deduced that a thrust bearing is likely to be turbulent if it has large diameter ($U = \Omega R$), low lubricant viscosity (such as water), high operating speed ($U = \Omega R$), and/or low load (large h). Although sometimes called flow instability, turbulence itself does not pose a threat to the bearing or the machine. It is very common in many applications and is not something that needs to be avoided. As a matter of fact, turbulence is beneficial for water lubricated bearings as it contributes to the bearing's load capacity (Armentrout *et al.* (2016)).

Due to the particles' fluctuating motion, turbulent flow demonstrates increased stress compared to laminar flow. Since stress is proportional to viscosity, turbulent flow can be treated as laminar flow with *effectively* increased viscosity. This increased viscosity is called eddy viscosity and is dependent on the flow itself (not a known material property). Using the effective viscosity, the Reynolds equation and the energy equation can be extended to model turbulence. There are two types of models to evaluate the effective viscosity. The first type is the bulk flow theory developed by Hirs (1973). In this theory, the averaged velocity across the thin film (bulk velocity) is directly correlated with the wall shear stress using an empirical drag law. At the end, the effective viscosity is calculated as a function of the local Reynolds number. The second approach is based on the "law of wall" theory for wall shear flow (Hinze (1975)). In this model, the eddy viscosity is assumed to be a function of the wall shear stress and the distance away from the wall. Eddy viscosity is zero in a viscous sub-layer very near the wall, and increases as the position moves from the wall to the core region of the lubricant film (Constantinescu (1959), Ng & Pan (1965), Elrod & Ng (1967), Safar & Szeri (1974)). The effective viscosity is then calculated as the superposition of the lubricant's material (dynamic) viscosity and the eddy viscosity.

The fluctuating motion of the fluid particles also enhances heat transfer across the thin film, leading to *effectively* increased heat conductivity. The added part due to turbulence can be calculated based on the eddy viscosity obtained above. Then, the effective conductivity is the sum of the lubricant's material conductivity and this added value. As discussed in Figure 14(a), the flow regime transition results in a dip on the temperature versus speed curve. That dip is the direct consequence of this effective heat conductivity. Of course, the increased shear stress (or effective viscosity) in turbulent flow also leads to more heat generation. Nevertheless, the net effect is the temperature reduction due to the more dominant effect of the enhanced heat transfer.

Figure 27 compares the maximum temperatures predicted with and without the turbulence model. The performance with turbulence considered have already been presented in Figure 14(a). As shown in this figure, laminar theory would substantially overpredict the maximum temperature in the turbulent flow regime. Not shown here, the power loss meanwhile would be greatly underpredicted. Therefore, the computer tool must have a good turbulence model in order to predict the performance of a thrust bearing operating in the turbulent regime.
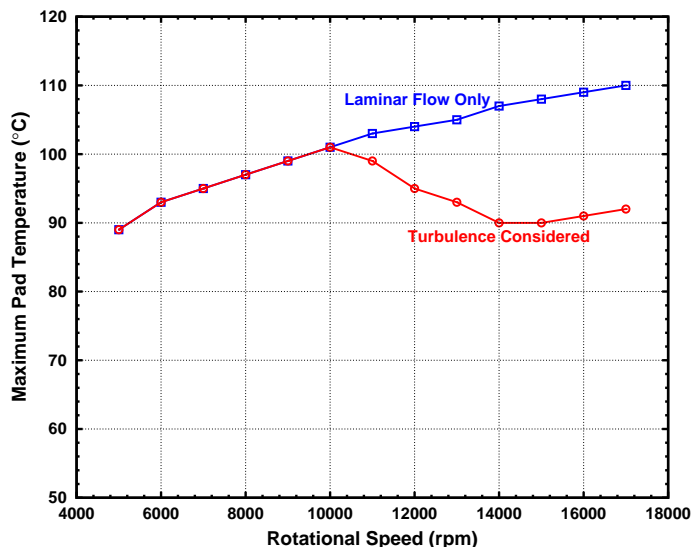
Figure 27: Pad temperature versus speed, comparison between laminar and turbulent theories

Power Loss and Drain Temperature

The shear stresses acting on the thrust collar form a resistive torque that consumes power. Since the fluid velocity has already been calculated for the energy equation, the shear stress on the collar surface can be easily obtained as viscosity times the velocity gradient. The power loss is subsequently calculated as $P = T \times \Omega$ where T is the integration of all the shear moments. Obviously, the resulting power loss only includes the viscous shearing on the active bearing side. The error can be quite large for a flooded bearing due to significant parasitic churning losses.

An approximate way to calculate the drain temperature is to apply a simple heat balance to the entire bearing. The rate at which heat enters the bearing is $\rho C_p Q T_S$ where Q is the oil flow rate through the bearing and T_S is the supply temperature. Inside the bearing, energy is added to the oil through viscous shearing at the rate of the power loss P. Consequently, the same oil has elevated energy rate of $\rho C_p Q T_D$ when leaving the bearing. Assuming no heat loss to the environment, the energy balance can be simply written as $\rho C_p Q T_S + P = \rho C_p Q T_D$, from which the drain temperature T_D is solved as

$$T_D = T_S + \frac{P}{\rho C_p Q} \tag{4}$$

The same control volume approach is often used to estimate the power loss in experiments. During testing, the supply and drain temperatures are measured, as well as the flow rate. The power loss is then calculated as $P = \rho C_p Q (T_D - T_S)$.

TEHD Algorithm

A theoretical analysis is performed to simulate various physical aspects and their interactions as illustrated in Figure 20. Assembling the models together, Figure 28 presents the flow chart of a comprehensive thermoelastohydrodynamic (TEHD) algorithm. As shown in this example, the computation begins with a set of initial values. The hydrodynamic pressure is calculated first by solving the Reynolds equation. The resulting mechanical deformation is immediately calculated and iterated with the pressure. In steady state conditions, the hydrodynamic force must balance the external thrust load, and the moment about the pivot must be zero if the pad can tilt. Therefore, another loop is used to iteratively determine the collar position and the pad tilt angle. The analysis so far involves elasticity and hydrodynamics and is called elastohydrodynamic (EHD) analysis. Please note that it is necessary to include the mechanical deformation in order to model the central pivot pad. Without it, the pad would have no load carrying capacity and the search for the steady state equilibrium would fail.

The next step is to include the thermal effects which are very important for typical applications. The film temperature is calculated from the energy equation while the pad and collar temperatures are obtained by solving the heat conduction. Local iteration loops are usually employed to ensure these coupled temperatures match and are consistent. Knowing the temperatures, the lubricant viscosity is updated and the thermal deformations can be subsequently included in the analysis. Since the analysis involves a hierarchy of iterations, numerical stability is an important practical concern for any computer software, in addition to its accuracy and capability. After all iterations reach convergence, the dynamic coefficients are calculated and the computer program prints out the results.
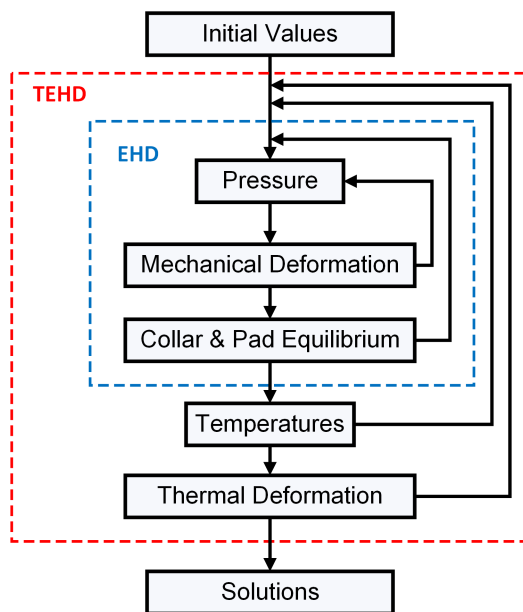
Figure 28: An example of a TEHD algorithm

Tremendous progress has been made since Osborne Reynolds, especially after the advent of the digital computer. Today, dedicated bearing software is widely used and provides an indispensable tool for analysis and design. However, there are still a number of limitations and challenges. To name a few:

- The temperature boundary condition at the leading edge. As discussed before, the physics is very complex and the prediction is usually based on simple models using empirical parameters. Physically, the inlet temperature is not a constant, but varies both axially and radially. It appears that CFD is necessary to achieve any significant improvement in the future, which requires significantly more computational resources. Direct lubrication designs further complicate this issue.

- The critical Reynolds numbers that control the modeling of the flow regime. The turbulence model generally works well for fully developed turbulence. However, the question is whether the bearing is physically turbulent, and thus, the turbulence model should be turned on. In analysis, the flow regime is controlled by two critical Reynolds numbers. The flow is treated as laminar if the actual Reynolds number is below the lower threshold. It is treated as full turbulence if the Reynolds number is above the upper threshold. If the Reynolds number falls in between, the flow is transitional and the eddy viscosity is scaled between 0 and 100%. Physically, the onset of turbulence is influenced by the bearing design and operating condition. It is difficult to accurately prescribe those critical Reynolds numbers since they are not universal. The prediction would have a large error if the bearing were modeled in the wrong flow regime.

- A large variety of pad geometries. Even though most pads are sector shaped, they can be different in details such as cutouts and surface crown. Those details can have strong influence on the bearing's performance and may need to be considered in the model. As a matter of fact, manufacturers sometimes tweak those details to achieve the desired performance. A general purpose computer program may not have the capability to model the exact details.

Given all those uncertainties, it is a good practice to benchmark the model whenever possible. The most likely available data are the temperature measurements during shop tests or field operation. Published experimental data of similar design and operation may also be used for correlation and model reconciliation. Such validation and reconciliation could significantly improve the accuracy and confidence in the predictions.

CONCLUSIONS

The key takeaways are summarized as the following:

- A thrust bearing has two operating limits: film thickness and temperature. The film thickness limit is related to the surface roughness and bearing size. The temperature limit is related to Babbitt creep and/or oil oxidation.

- To generate hydrodynamic pressure, there must be viscous lubricant, relative motion and a converging wedge. A bearing's performance is fundamentally dictated by these three ingredients.

- Thrust bearings can be classified as fixed geometry or tilting pad. Tilting pad bearings are typically used in high speed and/or high load applications. It can also be combined with self-equalizing mechanisms, which is required by some API specifications to compensate for static misalignment.

- The central pivot tilting pad usually relies on pad deformation to generate load carrying capacity. The load carrying capacity can be noticeably improved by increasing the circumferential pivot offset. Other important tilting pad bearing design parameters include surface crown, radial pivot offset and pivot design.

- Internal viscous shearing leads to temperature rise, which reduces lubricant viscosity, causes thermal deformation and imposes an operational limit. Effective ways to reduce temperature include increasing pivot offset, using chrome copper pads, upgrading to direct lubrication and/or evacuating the housing.

- For flooded operation, the supply flow rate must be sufficient to keep the oil bath acceptably cool. For evacuated operation, sufficient oil must be supplied to avoid severe starvation. Evacuated housing designs are often combined with directly lubricated bearings, which has the advantages of lower temperature and power loss. Care must be taken to protect direct lube bearings if there is a loss of supply flow.

- The thrust bearing usually does not have strong influence on the machine's lateral rotordynamics. However, it could be important when axial vibration or helical gear is involved.

- The Reynolds equation is the governing equation for the hydrodynamic pressure.

- The three-dimensional energy equation is used to model the film temperature. However, the film-pad-collar temperatures are coupled together, which usually requires iteration.

- Three dimensional pad deformation should be modeled, especially for a central pivot design whose performance is dependent on the effective crown.

- If it occurs, turbulence must be modeled since laminar theory would result in erroneous predictions.

- The user needs to understand the limitations of the computer tool. To improve accuracy, it is highly recommended to benchmark the analysis whenever possible.

NOMENCLATURE

A_P	=	Area of a single pad	(mm^2)
API	=	American Petroleum Institute	
C_p	=	Specific heat	$(J/(kg \cdot K))$
D	=	Diameter	(mm)
F	=	Force	(N)
h	=	Film thickness	(mm)
$\dot{m}$	=	Mass flow rate	(kg/s)
N_p	=	Number of pads	$(-)$
p	=	Pressure	(Pa)
P	=	Power	(kW)
Q	=	Volume flow rate	(m^3/s)
R	=	Radius	(mm)
T	=	Temperature or Torque	$(°C)$ or $(N \cdot m)$
u, v, w	=	Fluid velocity components in Cartesian coordinate system	(m/s)
U	=	Collar surface velocity	(m/s)
W_U	=	Specific or unit load	(MPa)
x, y, z	=	Cartesian coordinates	(mm)
β	=	Arc length from leading edge to pivot	$(°)$
θ	=	Pad arc length	$(°)$
κ	=	Thermal conductivity	$((W/(m \cdot K))$
λ	=	Hot oil carryover factor	$(-)$
μ	=	Viscosity	$(Pa \cdot s)$
ρ	=	Density	(kg/m^3)
τ	=	Shear stress	(Pa)
ϕ_c	=	Circumferential pivot offset	$(-)$
ϕ_r	=	Radial pivot offset	$(-)$
Ω	=	Angular velocity	(rad/s)

REFERENCES

API 610 (11th Edition), *Centrifugal Pumps for Petroleum, Petrochemical and Natural Gas Industries*, number STD 610, 2010 edn, American Petroleum Institute.

API 612 (6th Edition), *Petroleum, Petrochemical and Natural Gas Industries - Steam Turbines - Special-purpose Applications*, number STD 612, 2005 edn, American Petroleum Institute.

API 617 (8th Edition), *Axial and Centrifugal Compressors and Expander-compressors*, number STD 617, 2014 edn, American Petroleum Institute.

API 670 (4th Edition), *Machinery Protection Systems*, number STD 670, 2000 edn, American Petroleum Institute.

Armentrout, R., He, M., Haykin, T. & Reed, A. (2016), 'Analysis of turbulence and convective inertia in a water-lubricated tilting-pad journal bearing using conventional and cfd approaches', *Tribology Transactions* . Published online: 31 Oct.

Artiles, A. & Heshmat, H. (1987), 'Analysis of starved thrust bearings including temperature effects', *Journal of Tribology* **109**, 395–404.

Ball, J. (1996), 'Design considerations for thrust bearing applications', *Proceedings of the 25th Turbomachinery Symposium* pp. 223–241. Texas A&M University.

Brockett, T. (1994), Thermoelastohydrodynamic Lubrication in Thrust Bearings, PhD thesis, University of Virginia.

Capitao, J., Gregory, R. & Whitford, R. (1976), 'Effects of high-operating speeds on tilting pad thrust bearing performance', *Journal of Lubrication Technology* **98**, 73–80.

Constantinescu, V. (1959), 'On turbulent lubrication', *Proceedings of the Institution of Mechanical Engineers,* **173**, 881–900.

DeCamillo, S. (2014), 'Axial subsynchronous vibration', *Proceedings of the 43rd Turbomachinery Symposium* . Texas A&M University.

Dmochowski, W., Brockwell, K., DeCamillo, S. & Mikula, A. (1992), 'Study of the thermal characteristics of the leading edge groove and conventional tilting pad journal bearings', *STLE/AMSE Tribology Conference* .

Elrod, H. & Ng, C. (1967), 'A theory for turbulent fluid films and its application to bearings', *Journal of Lubrication Technology* **89**, 346–362.

Ettles, C. (1969), 'Hot oil carry over in thrust bearings', *Proceedings of the Institution of Mechanical Engineers* **184**, 75–81.

Gardner, W. (1988), 'Tilting pad thrust bearing tests - influence of pivot location', *Journal of Tribology* **110**, 609–613.

Gardner, W. (1998), 'Tilting pad thrust bearing tests - influence of oil flow rate on power loss and temperatures', *Proceedings of the 24th Leeds-Lyon Symposium on Tribology* pp. 211–217.

Grzegorz, R. & Michal, W. (2007), 'CFD analysis of the lubricant flow in the supply groove of a hydrodynamic thrust bearing pad', *Proceedings of ASME/STLE International Joint Tribology Conference* .

He, M., Byrne, J., Cloud, C. & Vázquez, J. (2016), 'Fundamentals of fluid film journal bearing operation and modeling', *Proceedings of the 1st Asia Turbomachinery and Pump Symposium* . Texas A&M University.

Heshmat, H. & Pinkus, O. (1986), 'Mixing inlet temperatures in hydrodynamic bearings', *Journal of Tribology* **108**, 231–248.

Hinze, J. (1975), *Turbulence*, 2nd edn, McGraw-Hill Book Company.

Hirs, G. (1973), 'A bulk-flow theory for turbulence in lubricant film', *Journal of Lubrication Technology* **95**, 137–146.

Martin, F. & Garner, G. (1973), 'Plain journal bearings under steady loads, design guidance for safe operation', *First European Tribology Congress* pp. 1–16.

Mikula, A. (1985), 'The leading-edge-groove tilting-pad thrust bearing: Recent developments', *Journal of Tribology* **107**, 423–430.

Mikula, A. (1986), 'Evaluating tilting-pad thrust bearing operating temperature', *Tribology Transactions* **29**, 173–178.

Mikula, A. (1988), 'Further test results of the leading-edge-groove (LEG) tilting pad thrust bearing', *Journal of Tribology* **110**, 174–180.

Ng, C. & Pan, C. (1965), 'A linearized turbulent lubrication theory', *Journal of Basic Engineering Ser. D* **87**, 675–688.

Pinkus, O. & Lund, J. (1981), 'Centrifugal effects in thrust bearings and seals under laminar conditions', *Journal of Lubrication Technology* **103**, 126–136.

Reynolds, O. (1886), 'On the theory of lubrication and its applications to mr. beauchamp towers experiments including an experimental determination of the viscosity of olive oil', *Philosophical Transactions* **177**, 157–234.

Rodriguez, P. (2000), Effect of tilting pad thrust bearings on rotor stability and forced response, Master's thesis, University of Virginia.

Safar, Z. & Szeri, A. (1974), 'Thermohydrodynamic lubrication in laminar and turbulent regimes', *Journal of Lubrication Technology* **96**, 48–56.

Simmons, J. & Dixon, S. (1994), 'Effects of load direction, preload, clearance ratio, and oil flow on the performance of a 200 mm journal pad bearing', *Tribology Transactions* **37**, 227–236.

Stewart, C. (1999), 'Influence of oil injection method on thrust bearing performance at low flow conditions', *Proceedings of the 28th Turbomachinery Symposium* pp. 133–140. Texas A&M University.

Suganami, T. & Szeri, A. (1979), 'A thermohydrodynamic analysis of journal bearings', *Journal of Lubrication Technology* **101**, 21–27.

Tower, B. (1883), 'First report on friction experiments', *Proceedings Institute of Mechanical Engineering* pp. 632–666.

Tower, B. (1885), 'Second report on friction experiments', *Proceedings Institute of Mechanical Engineering* pp. 58–70.

Whalen, J. (1996), 'Thrust bearing analysis, optimization and case histories', *Proceedings of the 25th Turbomachinery Symposium* pp. 17–24. Texas A&M University.

Wilcock, D. & Booser, R. (1957), *Bearing Design and Application*, McGraw-Hill Book Company.

ACKNOWLEDGEMENTS